



Faculty of Science and Technology

MASTER'S THESIS

Study program/ Specialization: Mechanical and Structural Engineering and Materials Science: Offshore Construction	Spring semester, 2013 Open / <u>Restricted</u> access
Writer: Lasse Steinmoen (Writer's signature)
Faculty supervisor: External supervisor(s):	S. A. Sudath C. Siriwardane Per Gunnar Bjoland
Title of thesis: Study of weld design and cost versus fabrication cost	
Credits (ECTS): 30	
Key words: Weld, notch stress, hot-spot stress, FEA, Solidworks, fatigue, weld fabrication	Pages: 54 + enclosure: 20 Stavanger, 17.06.2013 Date/year

0.0 Abstract

Increasing demand in economic- and time-efficiency, in the production and design phase, has led to the question if there is a possibility to save time and money on a more detailed analysis on which weld type to use.

The thesis tries to summarize the most important factors for the different properties of weld types regarding: strength, fatigue, risk, economical and manufacturing time.

The fatigue strength of steel connections is greatly reduced by the side effect of welds, which are structural stress concentration arising from the complexity of connection made possible by welds, local geometric stress concentrations at the transition between weld and parent material, and flaws in the metal produced by welding that are currently undetectable or unavoidable.

With the use of an example from Rolls-Royce Marine, where there was some discussion around the weld design, the fatigue strength for different designs were checked with the hot-spot method and notch stress method using finite element analysis in Solidworks, a 3D CAD program used in Rolls-Royce Marine, by:

- Comparing the results from the different weld types and stress assessment methods.
- Including risk management to decrease probability of failure.
- Check if or when necessary further analysis might be time saving, comparing the additional computing time for a more detailed analysis, versus the potential time saving on manufacturing.

The study found that in stiff structures, the hot-spot method might not manage to include the effect of stress concentration because of the weld itself. If in doubt, the notch stress method should be used.

Welds which are critical for the structures redundancy and in high risk environment should always be a full penetrating weld, to ensure fatigue cracking does not initiate at the weld root and trough the weld, which is hard to detect under an in-service inspections.

Comparing the cost of manufacturing and design analysis, the effect of cheaper weld design only comes in effect if the number of parts or components that have to be welded is large.

A suggestive flowchart for choosing weld type was made with respect to risk level and weld preparation cost versus engineering cost.

Contents

0.0 Abstract	2
1.0 Acknowledgments	5
2.0 List of symbols	6
3.0 Introduction	8
3.1 Background	8
3.1.1 Goal	8
3.1.2 Scope and limitations	8
4.0 Theory	10
4.1 Weld types	10
4.2 Fatigue	11
4.3 Factors reducing fatigue strength	12
4.4 S-N curves	20
4.5 Fatigue assessment	20
4.6 Nominal stress	21
4.7 Hot-spot/Structural stress	21
4.8 Notch-stress	23
4.9 Misalignment	24
4.10 Lamellar tearing	24
4.11 Considering risk	24
4.12 Non Destructive Testing	27
4.13 Fabrication time	28
5.0 Description of example	32
5.1 Load history for each down-hole operation:	35
5.2 Description of Soildworks	38
5.3 Modeling for Hot-spot:	39
5.4 Modeling for notch-stress:	41
5.6 Fatigue damage calculation	43
5.7 Risk analysis	46
6.0 Results:	47
6.1 Hot-spot results:	47
6.2 Notch-stress results	49
6.3 Estimating preparation time:	50
6.4 Through thickness properties:	51
7.0 Comments to Results	52
8.0 Conclusion	53

8.1 Flow chart for choosing weld type	54
8.2 Further work	55
9.0 References	56
10.0 Appendices	57
10.1 Appendix A: Stress extrapolation and fatigue damage calculations for Hot-Spot method	57
10.1.2 Weld design 1	58
10.1.2 Weld design 2	59
10.1.2 Weld design 2	61
10.1.4 Weld design 4	62
10.2 Appendix B: Stress extrapolation and fatigue damage calculations for Notch-stress method...	64
10.2.1 Weld design 1	65
10.2.2 Weld design 2	65
10.2.3 Weld design 3	66
10.2.4 Weld design 4	67
10.2.5 Weld design 5	68
10.2.6 Weld design 6	68
10.3 Appendix C: Through thickness reference table.....	70
10.4 Appendix D: Modeling of root for Fillet weld and Partial penetrating weld	71
10.5 Appendix E: Validation of notch-stress.....	71
10.5.1 Full-penetration cruciform joint	71
10.5.1 Fillet welded cruciform joint.....	72
10.6 Appendix F: Comparing stress types	73
10.7 Appendix G: Combination of T and P loads	74
10.8 Appendix H: Bad meshing.....	75

1.0 Acknowledgments

I would like to thank Rolls-Royce Marine Stavanger for their hospitality, the good food, coffee and tea. Special thanks to Per Gunnar Bjoland and Kjetil Dahl for helping when needed. Thanks to S. A. Sudath C. Siriwardane at UiS for guidance.

2.0 List of symbols

t = plate thickness

l = length

b = width

d = diameter

A = area

a = throat thickness

A_w = weld cross-section area

a_{eff} = effective weld depth

α = angle

P = vertical force

T = torque

$F_u(i)$ = Load function

$W_{traverse}$ = weight of traverse beam

$W_{topdrive}$ = weight of topdrive

n_p = number of pipes

$n_{p,max}$ = maximum number of pipes

W_p = weight of one pipe

L_p = length of one pipe

f_y = yield strength

f_u = ultimate tensile strength

Z_{Rd} = trough thickness resistance

Z_{Ed} = trough thickness load

Z_a, Z_b, Z_c, Z_d, Z_e = trough thickness properties

k_m = misalignment factor

σ = stress

$\Delta\sigma$ = stress amplitude

τ = shear stress

σ_n = nominal stress

σ_{hs} = hot-spot stress

σ_{ns} = notch-stress

σ_1 = 1st principal stress

σ_{max} = maximum stress

σ_{eff} = effective stress

$\Delta\sigma_C$ = detail category

$\Delta\sigma_D$ = constant amplitude fatigue limit

$\Delta\sigma_L$ = cut of limit

$\Delta\sigma_{max}$ = maximum stress amplitude

S-N = stress – cycle

m_1 = invers slope of S-N curve

m_2 = invers slope of S-N curve

$f(\Delta\sigma_R)$ = fatigue/S-N curve function

D = calculated fatigue damage/accumulated damage

N_i = number of cycles to failure at constant stress range $\Delta\sigma_i$

n_i = number of stress cycles in stress block i

i = block number

Σ = summation of

γ_M = Partial factor fatigue strength

γ_{Ff} = Partial load factor for fatigue limit state

t_p = preparation time

t_c = cutting time

Q_g = linear grinding rate

t_g = grinding time

API = American Petroleum Institute

DNV = Det Norske Veritas

BS = British Standards

Ec3 = Eurocode 3

IIW = International institute of welding

FAT = Fatigue Design Class

SD = standard deviation

CAFL = constant amplitude fatigue limit

DFF = design fatigue factor

Solidworks = 3D CAD program

NDT = Non Destructive Testing

CAD = Computer Aided Design

SCF = stress concentration factor

FEM = finite element model

FEA = finite element analysis

2D = two dimensional

3D = three dimensional

SF_d = API safety factor

3.0 Introduction

3.1 Background

There are currently no procedures in Rolls-Royce Marine for choosing which weld type to use at different connection scenarios. At this point it is done based on experience. In the construction phase and in the design phase, there is question whether there is time and money to be saved with a procedure for choosing weld types. There was also some discussion on a specific weld in a constructed 3D beam, whether the best design was used, and if the current design had led to a, strength wise, weaker beam.

The thesis is built up with a theory section, followed by a description of the mentioned example, description of Solidworks and the mesh modeling, analysis of the stresses at a specific weld in concern, comments on results and conclusion, references and appendices

- The theory section describes the different factors involved with the aspect of welding, from strength and fatigue to manufacturing cost.
- The description of the example explains how the beam is constructed, how the loading conditions are, and how they are transferred through the beam.
- The load history is explained, and the calculation method to incorporate the fatigue loading.
- Checking for alternative design using Solidworks for hot-spot method and notch stress method.
- Explaining how the modeling was done for the different assessment methods.
- The results are summarized and commented.
- A conclusion and a suggested flowchart was made.
- Most calculations and figures in the appendices

3.1.1 Goal

By summarizing the critical parts of weld design by the study of literature, research, different standards and looking into the details of the mentioned example. The thesis tries to suggest a procedure for choosing which weld to use at any time and suggest when a more detailed study might be necessary.

3.1.2 Scope and limitations

- Plate thickness lower than 50mm
- Standard offshore carbon steel, $355\text{MPa} \leq F_{y\leq} \leq 420\text{MPa}$
- Above sea
- NDT recommendations
- Risk assessment recommendations
- Design and FEA in Solidworks

Restricted to weld types:

- Fillet welds
- Partial-penetration welds
- Butt welds

The properties of these:

- Strength
- Fatigue strength
- Flaws
- Manufacturing properties

4.0 Theory

The chapters “Weld types”, “Fatigue” and “Factors reducing fatigue strength” is based on S. J. Maddox’s book “Fatigue Strength of Welded Structures 2nd edition”, where other sources and direct citation of the book, reference is used.

4.1 Weld types

Welds can be divided into two main categories, butt welds and fillet welds. A butt weld is a so called full penetration weld, typical butt joint shown in figure 1, and for static cases the joint is “as strong as the parent material” (1). A butt joint would produce a full strength joint.



Figure 1 Typical butt weld joint

Depending on the plate thickness, ends that are welded together require some preparation to ensure full penetration. This can make the weld quite complicated to complete. The preparation types are categories by letters based on the looks of the preparation type. Most common types are: I, V, U, X, half V, half X. V-butt weld to the left and X-butt weld to the right seen in figure 2 (2).



Figure 2: V-butt weld and X-butt weld (2)

Fillet welds are made by just attaching the plate/end together and weld as they are, and require no special preparation of the edges of the plates. Therefore fillet welds are much easier to make, they requires less skilled welders, less precision for fitting the members, cheaper to make and much more adaptable compared to butt welds.

Fillet welds can also be made partial penetrating. Then they will, however, require some end preparation to ensure sufficient penetration.

The load transfer in fillet welds are quite different from butt welds, the effective size of the weld is calculated from the throat thickness; a , which is the “shortest” theoretical thickness in the weld. And can be calculated as, for equally legged welds, the square root of the leg length. For unequal leg length, the definition of throat thickness is still the same, but the calculation is different. The static strength would be: $a * l * f_y$, where l is length of the weld and f_y is yield strength. Figure 3 (3) showing the definition of the different attributes of fillet welds.

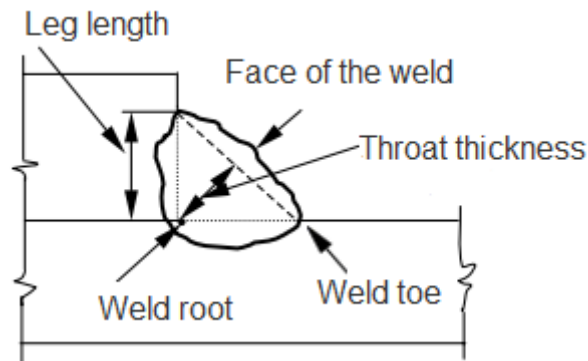


Figure 3 Typical fillet weld (3)

There are, of course, many different types of variation of these welds, and different types of welds used for other purposes than this thesis scope.

4.2 Fatigue

For fatigue, the capacity picture is a bit different. When metal is under repeated loading or variable loading there is a change in the micro structure of the metal. From the variation of stress in the metal, elliptical voids will start to grow from the impurity in the metal, like inclusion and void nucleation. Then straining between the voids, which eventually will start cracking and become a uniform crack (4) as seen in figure 4 (4).

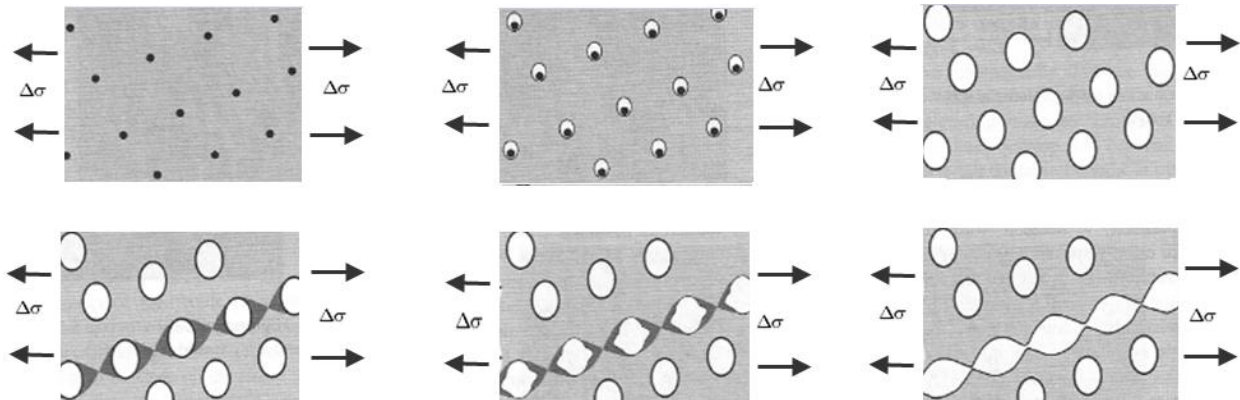


Figure 4: Crack growth from variable loading (4)

The magnitude of the variable stress, in a uniform plate, required to produce fatigue cracking is approximately 50% of ultimate tensile stress, or $140 + 0,25 \cdot F_u$ (3). Dependent on the stress amplitude, fatigue failure can happen after a few hundred cycles (high stress amplitude) or up to many million (low stress amplitude) cycles (1). Normally tensile forces have to be present for fatigue to be a problem, alternating stress from tensile to compression or alternating stress in only tensile state. This is normally expressed as an R value, where $R = \sigma_{\min} / \sigma_{\max}$ (5).

4.3 Factors reducing fatigue strength

A small change in the surface, for example a notch (small hole) in a plate, will cause the stress flow in the plate to change. And result in a stress concentration where the stress is higher than the average stress in the cross section. In a static loading condition, the excess area will hold the load, even though the area with stress concentration can suffer from plastic deformation. However, in a cyclic loading scenario the stress concentration can eventually cause the material to start cracking, and even further enhance the stress concentration. The crack will grow until section holding the cross section together is not large enough to hold the load, and plastic collapse will occur. As seen in figure 5 the fatigue life of the notched plate is slightly reduced and the fillet attachment will drastically reduce its lifetime.

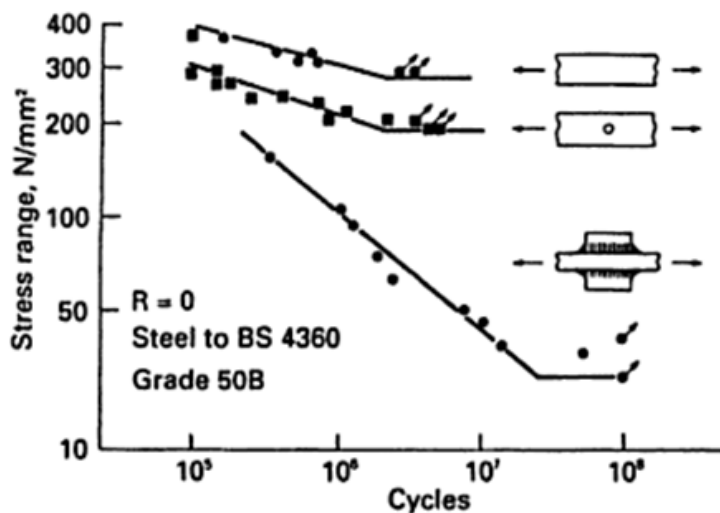


Figure 5: The effect on fatigue life of a fillet welded attachment versus a notched and a plain plate (1)

When a weld is introduced to for example a plate the weld bead will cause a disturbance in the force distribution, and a stress concentration is introduced. The change in stress flow after introducing a weld bead is shown in figure 6.

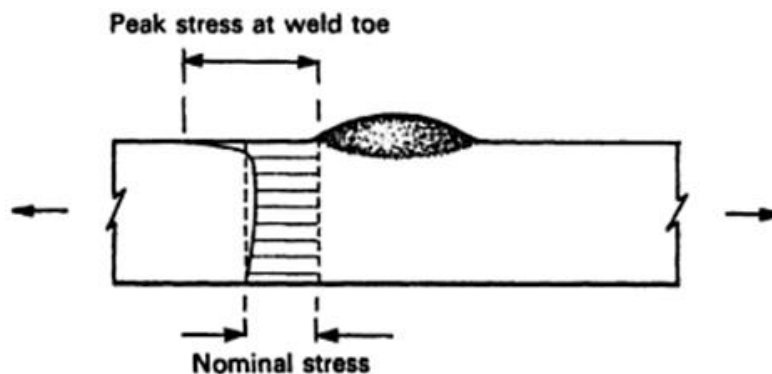


Figure 6: Stress concentration at toe of weld bead (1)

The stress concentration is even further enhanced if the transition between the weld and the plate is sharp, or “steep”, as shown in figure 7 (1) comparing a smooth transition in a butt weld (to the left) and sharp transition in a fillet weld (to the right).

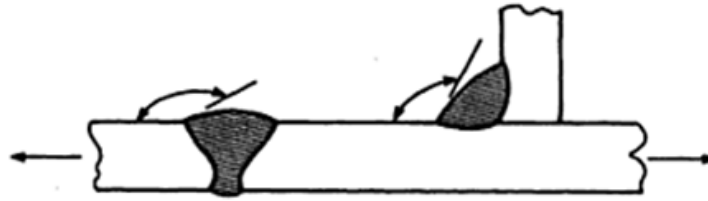


Figure 7: Smooth transition versus steep transition (1)

The effect of 45° and 30° transition on 1st principle stress in a FEA, in Solidworks, at the toe-notch is shown in figure 8 and figure 9, average stress is 100MPa.

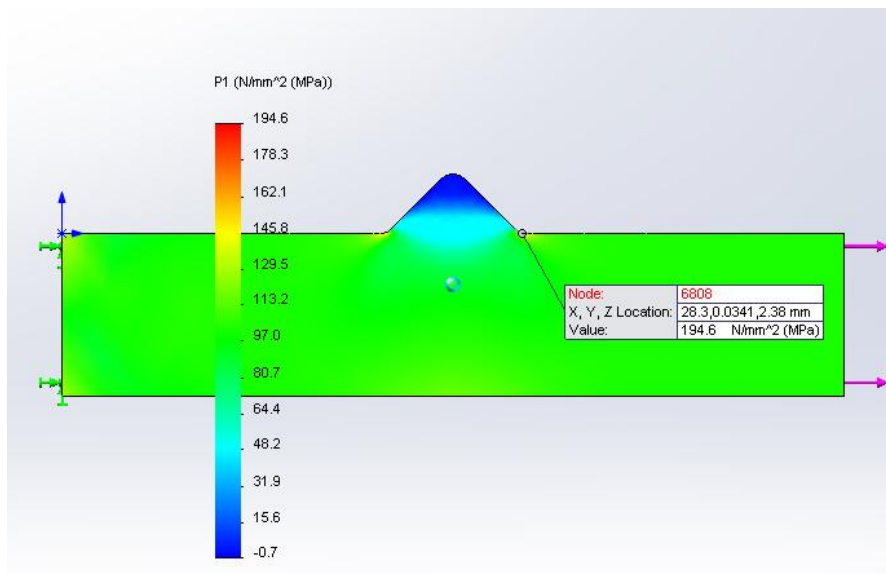


Figure 8: Notch stress at a typical fillet weld transition

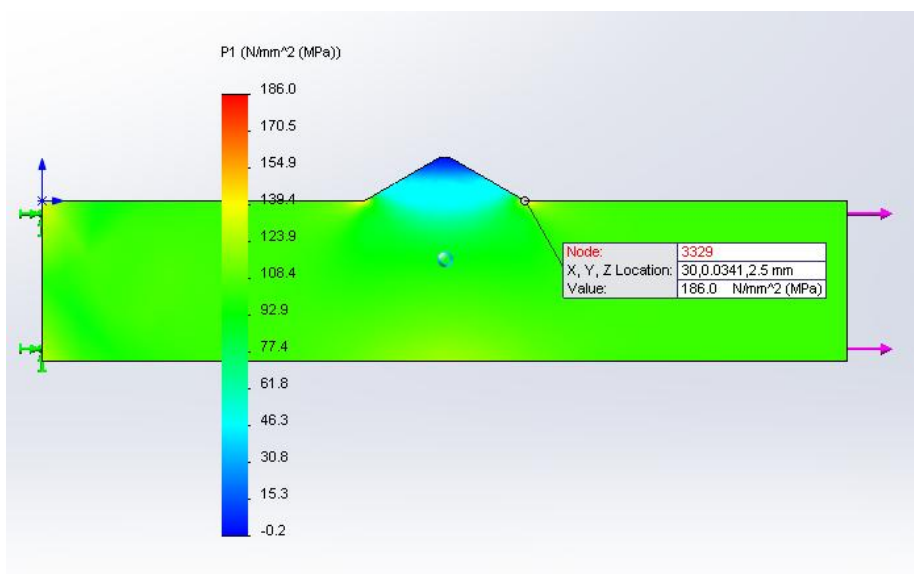


Figure 9: Notch stress at a typical butt weld transition

In relation to the welding, there is a chance of undercutting (a notch between the parent material and the weld toe, or root) and a small crack like feature called intrusion. For partial penetration welds and fillet welds there is also stress concentration at the root of the weld.

These problems occurs mostly in transverse welds (weld is perpendicular to load direction). When the weld is parallel to the load direction, discontinuities are a source of stress concentration. Start and stop positions are examples of discontinuities, also weld ripples, and fatigue cracks may start here, as shown in figure 10 (1).

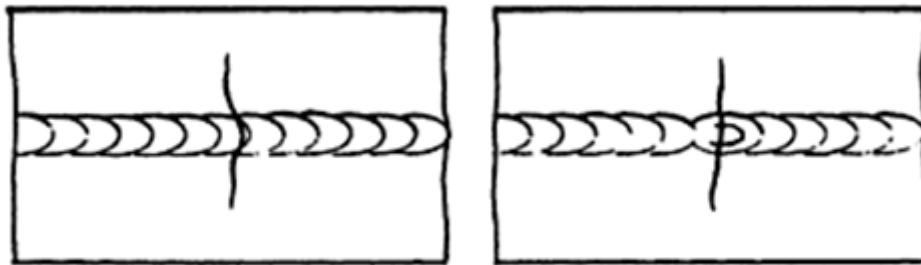


Figure 10: Fatigue crack start at a ripple (left) and at a start/stop position (right) (1)

There are also other flaws associated with the welding process. These include lack of fusion/weld root penetration, slag inclusion and porosity. If these flaws are causing a bigger stress concentration than the already mentioned factors causing stress concentration, they can be a source of initiating fatigue cracks. And they are most likely to be critical in joints with high fatigue strengths.

Since metals are melted together under welding, the material affected by the welding will be very hot and it will cool down afterwards. As known, metal expand when heated, and contracts when cooled down. Since the weld bead is in heated form, the volume of the cooled weld bead will be less than as welded, shown in figure 11; melted weld bead to the left and cooled to the right, this will cause compression forces away from the weld, and tension forces near the weld, referred to as residual stress.

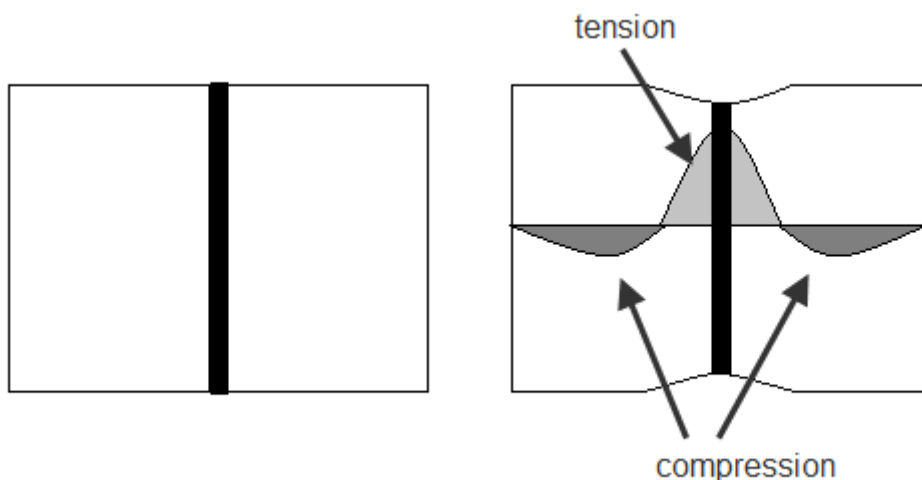


Figure 11: Compression and tension stress because of weld bead shrinkage

If the tensile stresses are larger than the compression forces in a joint, they have to be checked for possible fatigue damage. The intensity of these stresses is dependent on the nature of the joint, the main contribution from restraint of the combining plates, geometry, thermal properties and welding procedure. The stress can be as high as the yield strength of the material, this will lead to the effect called distortion. The effect of distortion is assumed to be the same as misalignment. The magnitude of distortion is assumed to be proportional to the size of the weld, and the eccentricity of the weld metal volume, shown in figure 12 large eccentricity of metal volume to the left and equilibrium of metal volume to the right.

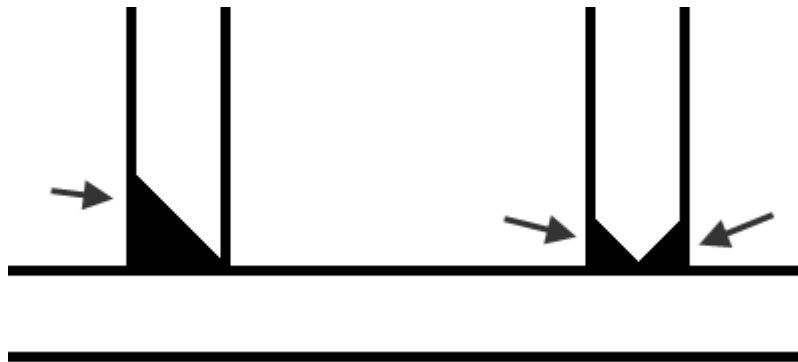


Figure 12: Large volumes of metal on one side versus equal volume on both sides

The magnitude of distortion can be calculated by certain FEM programs (6). One solution to this problem is the introduction of stress relieving measures, like preheating. The benefit from this treatment is mostly seen in specimens where there are partly or wholly compressive stresses, and only in high-cycle fatigue. For full tension stress there is a small variation in stress range, 15%, at $2 * 10^6$ cycles (1).

Given the welds are made in accordance with standards and checked with non-destructive testing, all these errors are incorporated in the design assessment method. The standard procedures usually takes care of problems like heat affected zone, hydrogen-induced cracking and deep undercutting.

Increase in the tensile strength of the weld material does not influence the fatigue life of a weld detail, the effect of higher ultimate limit strength of steel with and without weld on allowable stress range. Likely because of fatigue failures in welds are caused by crack like flaws, and there is no significant increase in crack rate growth in higher tensile strength of steel (1), although weld toe improvements show increase in fatigue life for higher strength steel (7). Weld toe improvements are physical intervention done to the weld toe after welding, like grinding down cracks and smoothing the transition between the weld and parent material.

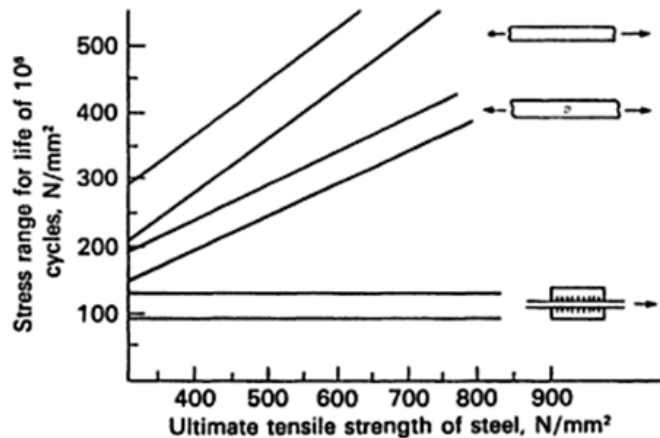


Figure 13: Effect of higher strength material with fatigue in mind (1)

If there is misalignment of plates, when transverse of the load direction, it will cause an eccentric bending moment, and increase the stress in the joint (1). Unless the load in the joint is only bending, this will reduce the fatigue strength of the joint (1).

The stress concentration effect is also depending on the relative size between the weld and the welded plate. The effect is largest when the stress concentration at the surface is the source of fatigue crack (weld toe). For welded attachments it is found that the stress concentration increases with the length of the attachment and the thickness of the plate which the attachment is welded onto (1). This can be transferred to include butt welds, where the weld bead length is compared to the attachment length.

In a transverse butt weld, the weld will create a source of stress concentration in the joining plates. The fatigue strength of a joint is reduced quite drastically. And the fatigue failure will occur beside the weld, at the weld toe, or in the weld, not in the parent material. The smoother the transition between the parent material and the weld, the better fatigue properties of the welded joint will have. Poor profile and sharp transition in the weld, because of higher stress concentration, will reduce the fatigue strength of the weld. This is why excess weld metal should be avoided, and “weld reinforcement” is in fact not making the weld stronger, and should be described as “overfill”.

Full penetration welds is usually made from two sides, to get full control of the weld profile. But in some cases there is only access from one side. This may result in a poor root quality. Lack of root penetration, abrupt profile, misalignment and cracks in the root area can easily happen. This will be a source for the fatigue crack to initiate, and reduce the fatigue capacity.

A normal solution to this problem is the use of a permanent backing strip. The weld will fuse with the backing strip, and will make a smooth weld root. However, there will be a high stress concentration at the fuse between the weld metal and the backing strip. This new source of stress concentration will cause the fatigue crack to initiate at this point, and grow trough the weld. This reduction in the fatigue strength puts the weld almost to a level of a fillet weld, but this may be a small price to pay for a full penetration weld, for example in a pipe.

For longitudinal butt welds, the edge of the weld will not be a source for stress concentration. The properties causing stress concentration in the longitudinal butt welds are the ripples in the weld, and the start/stop position caused by for example changing electrode in manual welding. The corresponding stress concentration factor is far less than the stress concentration associated with the edge of the weld in a transverse weld.

The result is higher fatigue strength for longitudinal butt welds, than transverse butt welds. Similarly, for welds made from one side, incomplete penetration will no longer be a source of stress concentration. The main problem for this type of weld is the variation in the root bead, usually resulting in higher stress concentration than the ripples caused by the welding. A permanent discontinuous backing strip will not cause a stress concentration in a longitudinal direction, therefore a good solution to this problem. The backing strip should be connected using a continuous fillet weld (1).

One butt welded joint which should be avoided, is the connection between one plate, which is under stress, and side plates. This causes a quite large stress concentration, and the weld further enhances this effect. (1)

The nature of the design and form of the fillet weld will produce a high stress concentration, and will have significantly reduced, especially load carrying welds, fatigue strength. Just the use of attachments, like gussets, cover plates, brackets etc., will disturb the stress flow in the load carrying part, just like in a butt joint there will be a possibility of fatigue crack growth near the toe or root. Since permanent offshore environments are subjected to extensive variable loading, only fillet welds which are non-load-carrying is likely to be used.

As mentioned, because the weld causes a disruption in the plate surface, fillet welds will cause stress concentration even if there is no load transfer. The stress concentration increases at the weld toe or end increases with the size of the weld. The length of the weld is the most critical attribute regarding weld size, also the thickness of the edge of longitudinal attachments or width. The thickness of the main plate also contributes to the fatigue strength of fillet welds. For transverse attachment, welded with double fillet weld, the weld toe is the highest source of stress concentration, and fatigue cracks will start at one of the toes. The weld can have a convex shape or a concave shape. A convex shape will generate a larger throat thickness, but there is a higher chance of undercutting and because of the steeper transition between the weld and parent material the stress concentration is higher. Therefore a convex shape is preferred for static structures (1). For structures under fatigue loading, a concave shape is desirable, because of lower stress concentration. However, the concave weld is more prone to shrinkage and cracking (3).

In single sided fillet welds there is stress concentration at the weld toe and root. And fatigue cracks may initiate from both. Fatigue cracks starting at the root are very unlikely to be detected before failure. There is also no help in toe preparation, to reduce the risk of fatigue crack initiation.

For welds parallel to the stress direction, the crack will start at the end. Therefore there will be no increase in fatigue strength. Large plate attachments will also reduce fatigue strength. Intermittent fillet welds will have a lower stress concentration, and have higher fatigue strength. The fatigue properties of load-carrying-fillet welds are very poor, because of high stress concentration at the root. Figure 14 showing the stress concentration, calculated by FEA, at the toe and root of a load carrying fillet weld with nominal stress of 100MPa.

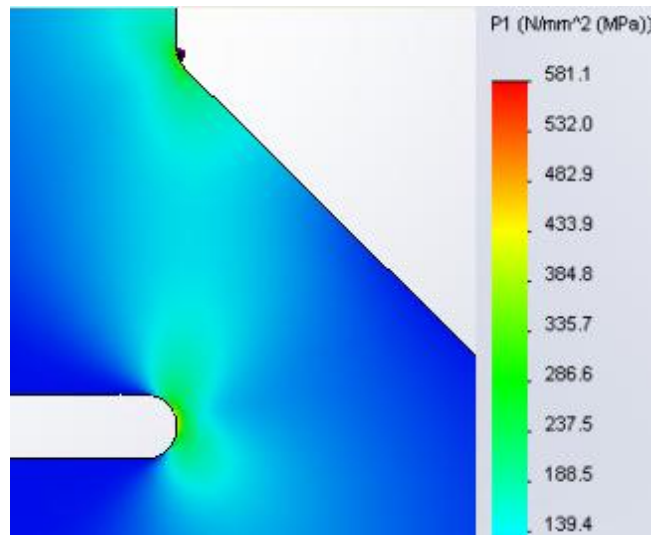


Figure 14: Load-carrying fillet weld with stress concentrations

For load-carrying fillet welds, the stress flow is quite different from butt welds. As mentioned the force, P , have to be divided by the smallest area in the weld. This is defined by the throat thickness of the weld. Assuming a 45° weld, the throat thickness would be the square root of the leg length. And the area of the weld, A_w , would be length of the weld times throat thickness, $A_w = l * a$, and allowable load would be two times A_w times f_y , $P = 2 * A_w * f_y$, for fillet welds on both sides of the load-carrying plate, single sided fillet welds should be avoided. Depending on the ratio between the area of the plate(s) and area of the weld, the nominal stress in the weld can either be higher, equal or lower than the nominal stress in the plate. (1) This ratio is normally expressed as; $2 * \frac{A_w}{A}$, and called design ratio (1).

For fatigue loading this disturbance in the force flow will make the design of the fillet welds a bit harder. Many shapes and configuration can be used, all of which show slightly different fatigue strength and failure modes (1). By looking at the two of the most usual types of joint, the factors involved can be found. Closer examination of the stress flow in the cruciform joint shows that there are two sources of stress concentration, weld toe and weld root (1). With the two sources of stress concentration, the problem is knowing where the fatigue crack will initiate. Decreasing the leg length will not severely increase the stress concentration at the toe (1). However, the stress in the weld will increase, and the stress concentration at the root will increase, causing the crack to start here. The opposite can happen if the leg length is increased, the crack may start at the weld toe (1). Therefore the failure mode of the weld is dependent on the ratio of the leg length and plate thickness. And the best leg length would be when the ratio is so that the crack would start at the weld toe. The general result is that the leg length should be equal to the plate thickness. Therefore a thicker plate would require larger weld. For thick plates this might be a problem, and partial penetrating weld might be a solution. DNV have made a figure (8) describing the effect of the different parameters in relation to toe and root cracking (figure 15).

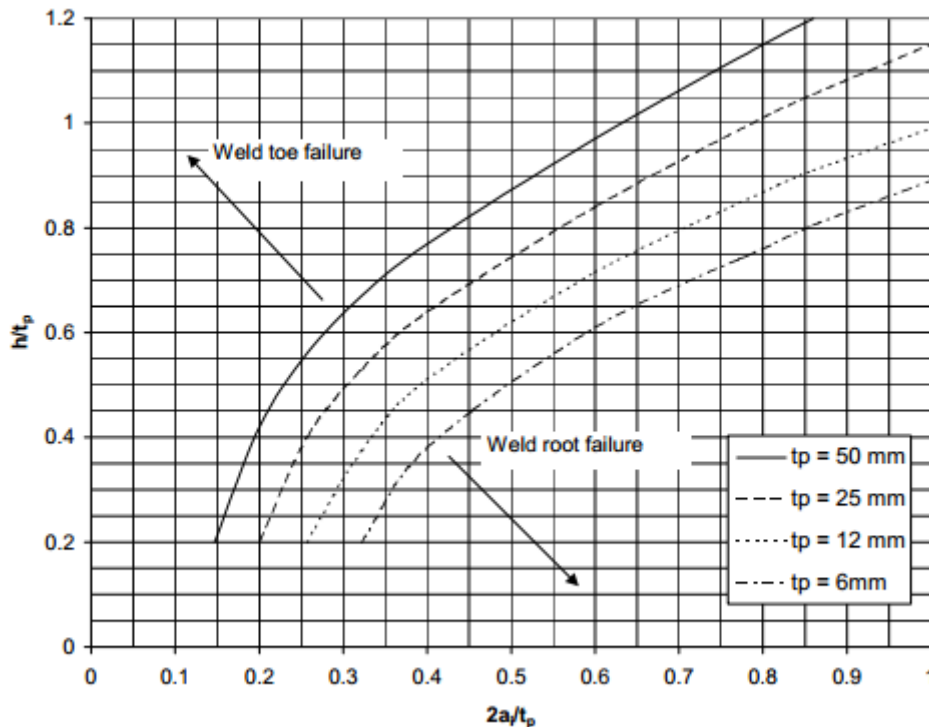


Figure 15: Relation between the distance between the load carrying weld roots, $2a_i$, and the leg length of the weld, h . Dependent on t_p , which is plate thickness (8)

An increase in weld area above the optimum design area, by larger weld or partial penetration welds, will not increase the fatigue performance (1). Only a full penetration weld would do so. Even this would just slightly increase the allowable stress for fatigue life.

Cruciform joints will also suffer from misalignment.

If we look at a fillet welded T joint, the failure modes will be quite similar to the failure mode of cross joint, but it will also introduce a third mode of failure if the transverse member is under bending, toe crack in the attached member (1).

For longitudinal load-carrying fillet welds the weld toe (like full penetration welds) and root become parallel to the stress. But like the attachment plates, the weld ends will create a source of stress concentration, i.e. intermittent fillet welds in a web to flange connection or a double lap joint (1).

For a double lap joint connection the welds on the edges on a loaded plate can be more dangerous than the welds on the surface of the plate. Therefore the weld should be made continuous all around the plate.

In addition to the stress concentration introduced by the weld itself, there can also be a severe stress concentration in the structural design. A good example for this is a hole in a plate. Without the hole, the nominal stress will be load divided by the net section area. Introducing the hole, the new net section area would be width minus hole-diameter multiplied with the thickness. And the structural stress near the hole could be up to three times larger than the nominal stress (1).

4.4 S-N curves

The most common method used in standards for ensuring sufficient fatigue strength is the use of S-N curves, where S is stress and N is fatigue life in number of cycles (7). It is based on statistical analysis of fatigue test data from welded joints, and the results produce a mean S-N (7). The relationship between $\log(S)$ and $\log(N)$ is assumed to be a straight line (7). The standard deviation, SD, of $\log(N)$ is also calculated, which indicates the uncertainty in the mean curve (7). The design curves are calculated with the mean curve minus two standard deviation, which would give a confidence level of 95.4%, where the lower part of the remaining 4.6 %, is 2.3%, which represent the probability of failure (7). Or 97.7% probability of survival. A curve based on three times standard deviation will produce a 99.9% probability of survival. Most standards use a 97.7 % probability of survival, for example IIW, DNV, Ec3, ABS and BS.

The design S-N curves are based on a general equation relating applied stress range, S and fatigue life N (1):

$$S^m * N = a * \Delta^d$$

Where S is stress, m is the slope of the $\log S - \log N$ curve, N is the number of cycles, a is a constant which refers to the mean S-N curve, Δ depends on the standard deviation of $\log N$, sigma, such (1);

$$SD = \log \left(\frac{1}{\Delta} \right)$$

And d is the number of standard deviations from the mean curve, d is set to 2 in standards (1).

For fatigue assessment of welded joints, S-N curves are represented by a two slope curve, where the inverse slope of the curves is represented by m_1 and m_2 (7). Usually $m_1 = 3$ and $m_2 = 5$ (7). Where the two slopes interfere is called the constant amplitude limit (9), which is set to 10^7 in DNV (8) (in air) and IIW (9), and $5 \cdot 10^6$ (10) Ec3. And cut of limit is set to 10^8 , the damage of the variation of stress under this limit is neglected. These changes in the slope of the curve are often referred to as knee points.

4.5 Fatigue assessment

Fatigue assessment with the use of S-N curves is normally based on assumption of linear damage accumulation and, for variable amplitude loading, assessed with the "Palmgren-Miner"-rule, or modified version of this rule (9).

$$D = \sum_1^i \frac{n_i}{N_i} \leq 1$$

Where D = accumulated damage

I = index for stress block number in load

n_i = number of stress cycles in stress block i

N_i = number of cycles to failure at constant stress range $\Delta \sigma$ i

However, this rule is not recommended for very high number of loads.

For stress cycles under the constant amplitude knee point ($N < 10^7$) research indicates failure at $D = 0.5$, and for stress spectra with high mean stress fluctuations, $D = 0.2$ (9).

There are three different methods common in standards for defining the stress used with these S-N curves. Nominal stress, structural stress (hot-spot-stress) and notch stress. Where nominal stress is based on simple beam theory, hot-spot stress is extrapolation of stress near the weld by finite element method or strain testing (9) and notch stress is extrapolation of stress at the weld toe by finite element method or the use of different theories for stress concentrations (5).

The chapters “nominal stress”, “hot-spot/structural stress” and “notch stress” is based on “DNV-RP-C203” and “IIW-1823-07 ex XIII-2151r4-07/XV-1254r4-07”

4.6 Nominal stress

The definition of nominal stress is the average stress amplitude over the cross section area.

$$\sigma_n = (P_{\max} - P_{\min})/A$$

For fillet welds and partial penetration welds the nominal stress is the stress in the weld, cross section area is then the total area of weld(s), $A = A_w = l * a$.

The different joints resulting in the different S-N curves are divided into joint-categories. There are up to eleven main categories which are often represented by letters, A, B, C, D, E, F1, F2, G, W, W2, W3 (DNV), or FAT # (Ec3 and IIW), where the number represents stress limit for $2 * 10^6$ cycles, i.e. FAT 100 have a fatigue strength of nominal stress at 100 MPa in $2 * 10^6$ cycles.

The geometric stress concentration and the allowed weld flaws are taken into the class system. In the test data, most of the joints have been under one directional load, axial and/or bending, and the nominal stress is quite easy to calculate. Where the stress picture is more complex, the maximum principle stresses are used. Shear stresses should also be considered (9)IIW.

Most details with geometric stress concentration near the weld, i.e. weld near a hole, are covered in the classification system. However, different types joints may not be covered, and the local structural stress concentration have to be considered (1).

It should be noted that some misalignment and flaws have been incorporated in these curves. (9). The magnitude of the misalignment of the finished weld should be checked after the standard used (8).

4.7 Hot-spot/Structural stress

For complicated welded structures the special connection can make the nominal stress in the weld area hard to define (5). The use of structural stress or hot-spot stress by finite element model may be a good alternative to nominal stress.

The hot-spot method includes the modeling of the geometric stress concentrations, by extrapolation of the stress at a certain distance from the weld and interpolating the hot-spot stress, shown in figure 16 (8).

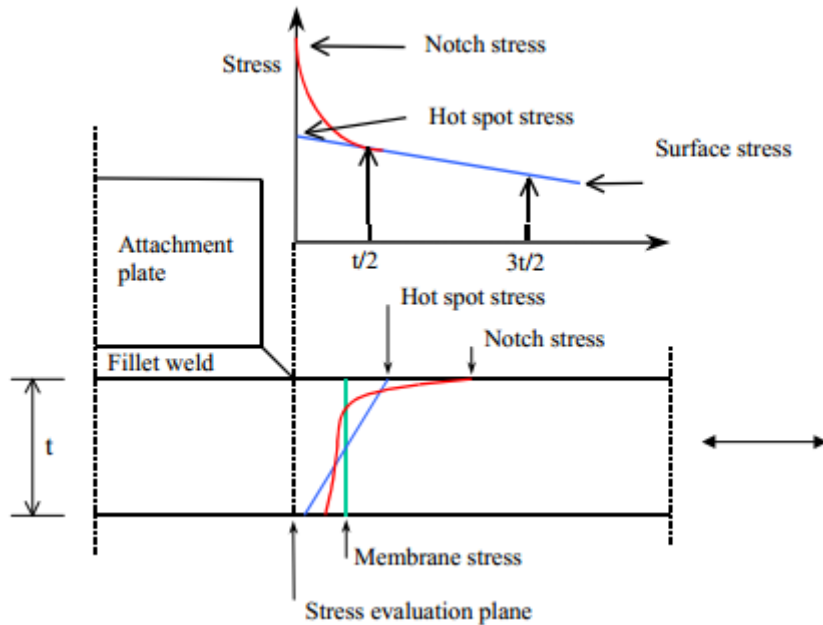


Figure 16: Definition of hot spot stress by interpolation (8)

The local stress concentration, or notch, is included in the design S-N curve. DNV recommends the D-curve/FAT 90 and stress extrapolation at distances of $0.5t$ and $1.5t$ from the weld toe (8). Ec3 and IIW uses joint classifications to some degree for hot spot stress as well, Ec3 uses curves from FAT 90 to FAT 112 and IIW uses FAT 100 and FAT 90. IIW recommends distances of $0.4t$ and $1.0t$, Ec3 is quite unclear which stress to use. E. Niemi recommends FAT 90 for load carrying welds and FAT 100 for non-load carrying welds and recommends stress extrapolation at $0.4t$ and $1.0t$ away from the weld toe (7).

The 1st principal stress is usually the stresses to be used (9). DNV have formulas for which stress to use, to incorporate large shear stresses.

Different types of hot-spot stresses are defined. DNV defines 3 spots and IIW define 2. DNV (figure to the left) uses a, b, and c, where a) is at the weld toe on the plate surface at an ending attachment, b) at the weld toe around the plate edge of an ending attachment, c) along the weld of an attached plate (8). For IIW, a) weld toe on plate surface and b) Weld toe at plate edge. Where a) and c) is dependent on plate thickness. (9)

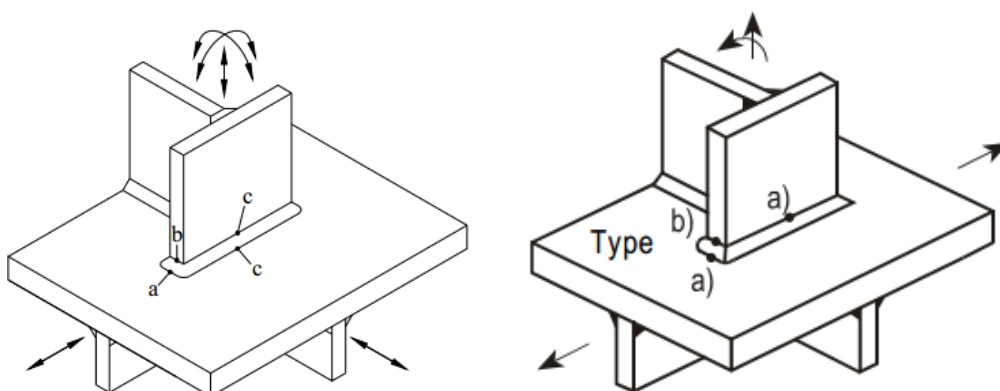


Figure 17: definition of hot-spots according to DNV (8) (left) and IIW (9) (right)

This method is only applicable for evaluation of the weld toe, potential root crack should be checked by appropriate nominal stress curve or notch-stress method (9).

For complex 3D models with solid elements both IIW and DNV recommends a 20 node element for element sized equal to plate thickness, and one layer of elements in the thickness direction is sufficient. DNV also has recommendation for 8 node elements, and suggests element size of 0.25t and at least 4 layers of elements.

In the model, the transition between the “main” elements and the finer elements in the hot-spot region should have a fine transition between the two. And the elements in the hot-spot region should be carefully evaluated with respect to its geometry, i.e. corner angles between 60 and 120, and a length breath ratio of maximum 1 to 5 (8).

Also the model should be large enough so there is as few as possible assumptions made regarding the boundary conditions (8).

The model should be as close to reality as possible (9), (8). Since the geometry in the model is idealized, the possible effect of misalignment has to be considered, multiplying the stress with a misalignment factor according to IIW or stress concentration factor according to DNV. Although a factor of 1.05 have already been included in the S-N curves (9).

4.8 Notch-stress

Another method for incorporating the geometric stress concentration and weld geometry for complicated structures is the use of the notch-stress method (5). The finite element method approach requires some extra modeling time and more computer power to calculate compared to the hot-spot method.

Notch-stress is the maximum stress in an artificially created notch with 1mm radius, usual 1st principle stress (7), at the weld toe or root, and this stress is used with an S-N curve. Because of the scatter in weld geometry and imperfections caused by welding, and weld flaws which is undetectable by current non-destructive examination standards, it is recommended to use the FAT 225 curve (9), although one study recommend FAT 200 curve for thinner sections ($t \leq 10\text{mm}$) and FAT 300 for different weld improvement methods (11), another suggest FAT 300 for specific welds (12). As the hot-spot method, some unavoidable misalignment is incorporated in the FAT 225 S-N curve, which is set to 1.05 (9).

For the modeling for the finite element analysis there should be designed a perfect weld with a notch with radius of 1mm at the end of the weld toe or root. If not stated, butt welds should have a 30° transition and fillet welds should have 45° transition to the welded plate (9) (8). DNV recommends element used around the notch should be the sized so that there are at least four elements around the quarter of the notch radius. And the elements should remain unaltered for at least 3 layers of elements. IIW recommends elements size of maximum $\frac{1}{4}$ of the notch-radius for higher order elements, which would be 0.25 mm (9). The size should be inspected after meshing, and should be observed in the curved part of the notch and the beginning of the straight part right in front of the notch (9).

As the radius of the notch decreases, and therefore the elements size should decrease, the associated notch stress would increase (9).

If there is doubt if the elements which is used, there should be made a validation model, where the results can be compared with knows methods, for example nominal-stress method (8).

This method is limited to plate thickness as large, or lager, than 5 mm. For smaller thicknesses, there have been studies shown that a notch radius of 0.05mm and a FAT 600 curve could be used (13). Should be noted that the stress concentration factors can be calculated by formulas (9).

4.9 Misalignment

The effect of misalignment is dealt with by introducing a factor which is multiplied with the stress calculated (8) (9). For IIW this is called k_m and DNV uses SCF. For hot-spot and notch-stress there is already included a k_m of 1.05 in the S-N curve, and for nominal stress approach this varies from 1.15 for butt joints to 1.45 from cruciform joints (9). IIW also suggests a default value to be used with the hot-spot and notch-stress approach, 1.1 for butt joints and 1.4 for cruciform joints (9). The misalignment effect should be calculated after the standard used.

4.10 Lamellar tearing

Lamellar tearing, displayed in figure 18 (14), or through thickness strength, is the strength a material have against internal tearing of the material when the weld metal shrinks (14). It is mainly of concern when the weld is on the surface of a plate, for example corner joints, T joints and cruciform joints (14). In Ec3 it is covered by giving steel a given material coefficient for its strength against lamellar tearing, Z_{rd} (14). The effect can be neglected if $Z_{Ed} \leq Z_{Rd}$, where Z_{Ed} is a summation of criteria that effect lamellar tearing. (14). Formula from Ec3 (14):

$$Z_{Ed} = Z_a + Z_b + Z_c + Z_d + Z_e$$

These are effective weld depth, shape and position of joint, thickness of material welded on, restraining conditions and heat of material when welding, which is explained in Ec3 (14)

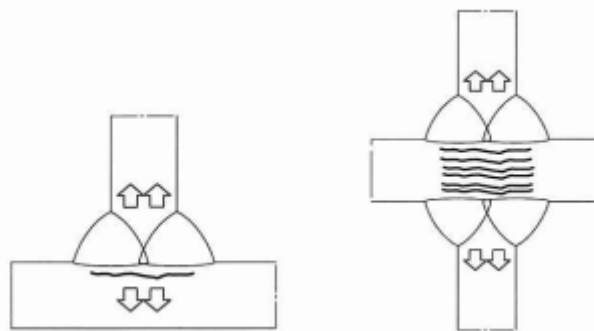


Figure 18: Lamellar tearing in T joint and cruciform joint (14)

4.11 Considering risk

Risk is commonly defined as the probability of failure versus the consequence of failure, or Risk = Consequence*Probability. To handle the risk, first the consequences of failure should be evaluated, and then design should be made after this evaluation to get sufficient survival probability. This is usually done by a risk matrix, typical risk matrix in figure 19.

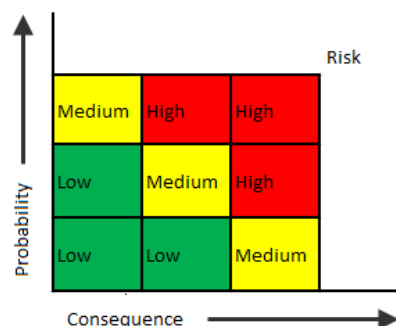


Figure 19: Typical risk matrix

The onshore based recommendations IIW and Ec3, recommend using a factor on the design curve to ensure sufficient risk control. Table 1 shows IIWs recommendations (9)

Table 1: Showing IIW recommendations for γ_m (9)

Partial safety factor γ_M → Consequence of failure	Fail safe and damage tolerant strategy	Safe life and infinite life strategy
Loss of secondary structural parts	1.0	1.15
Loss of the entire structure	1.15	1.30
Loss of human life	1.30	1.40

In contrast the offshore based recommendations DNV and ABS, recommends using a Design Fatigue factor, which is multiplied by the accumulated damage. These standards also considers if the risk is manageable after construction, by for example routine NDT inspections. Table 2 (15) suggests different DFF (here Fatigue Design Factor) for different types of structural components, also there is a footnote for uninspectable structural details DFF should be 5 for ordinary and 10 for critical components (15).

Table 2: Table from ABS showing recommended DFF for different types of structural details (15)

TABLE 1
Fatigue Design Factors for Structural Details**

** The minimum Factor to be applied to uninspectable 'ordinary' or uninspectable 'critical' structural details is 5 or 10, respectively.

STRUCTURAL DETAIL ⁽³⁾		GOVERNING FATIGUE STRENGTH CRITERIA	APPLICATION ⁽¹⁾ CATEGORY**	
LOCATION	Type		ORDINARY	CRITICAL ⁽²⁾
Structural Subsystem ⁽⁴⁾				
FIXED & FLOATING INSTALLATION				
ABOVE WATER STRUCTURE				
Non-Integral Deck ⁽⁵⁾	Non Tubular ⁽⁷⁾	ABS-(A)	1	2
	Tubular Intersection ⁽⁸⁾	ABS-T(A)	1	2
Integral Deck ⁽⁶⁾	Non Tubular	ABS-(A)	2	3
	Tubular Intersection	ABS-T(A)	2	3
IN WATER & SUBMERGED STRUCTURE ⁽⁹⁾				
Fixed Non-Floating Structure (e.g. fixed jacket, tower and template)	Non Tubular	ABS-(CP) ⁽¹⁶⁾	2	3
	Tubular Intersection	ABS-T(CP) ⁽¹⁶⁾	2	3
Fixed Floating Structure (e.g. TLP, Column Stabilized & SPAR; but excluding Ship-type & MODU ⁽¹⁴⁾)	Non Tubular ⁽¹⁰⁾	ABS-(CP)	3	5
	Tubular Intersection	ABS-T(CP)	3	5
FOUNDATION COMPONENTS ⁽¹²⁾		ABS-(CP) or ABS-T(CP)	NA	10
MOORING COMPONENTS ⁽¹³⁾		ABS FPI Guide ⁽¹¹⁾	NA	3
TLP TENDON ⁽¹³⁾		See Note 15	NA	10

DNV have also illustrated the probability of fatigue failure after calculated fatigue damage, D , shown in figure 20 (8).

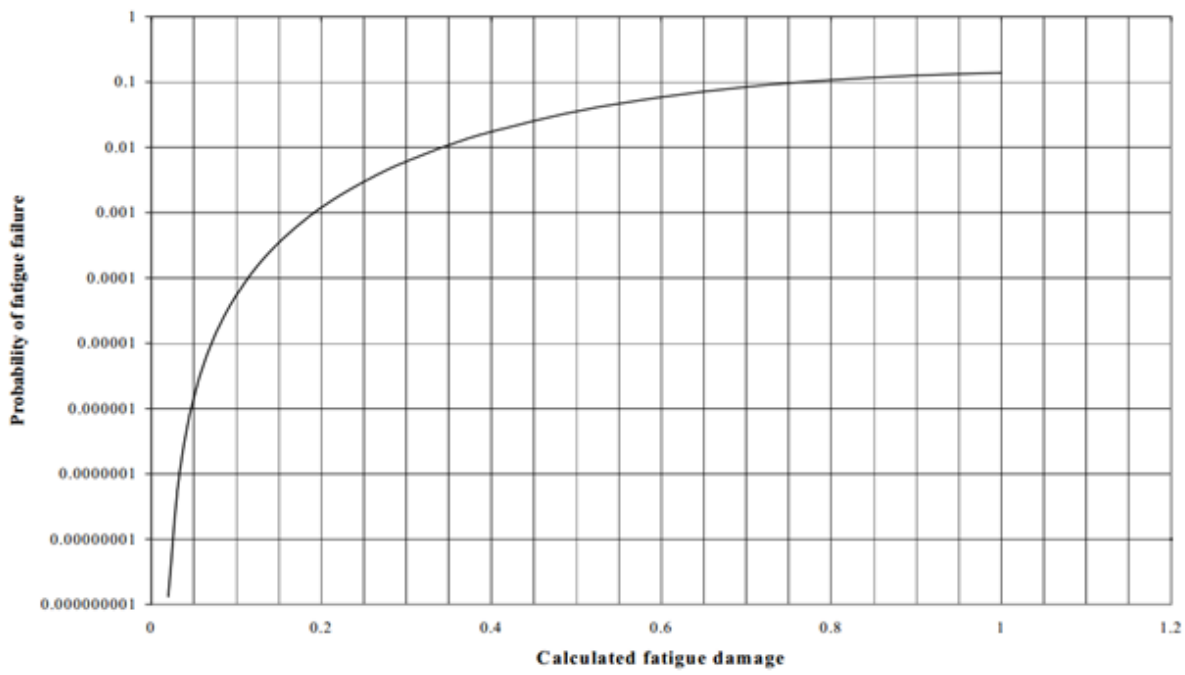


Figure 20: Probability of failure according to calculated fatigue damage (8)

The effect of DFF on probability of failure is shown in figure 21 (8), where failure probability is shown with reference to annual probability and accumulated probability.

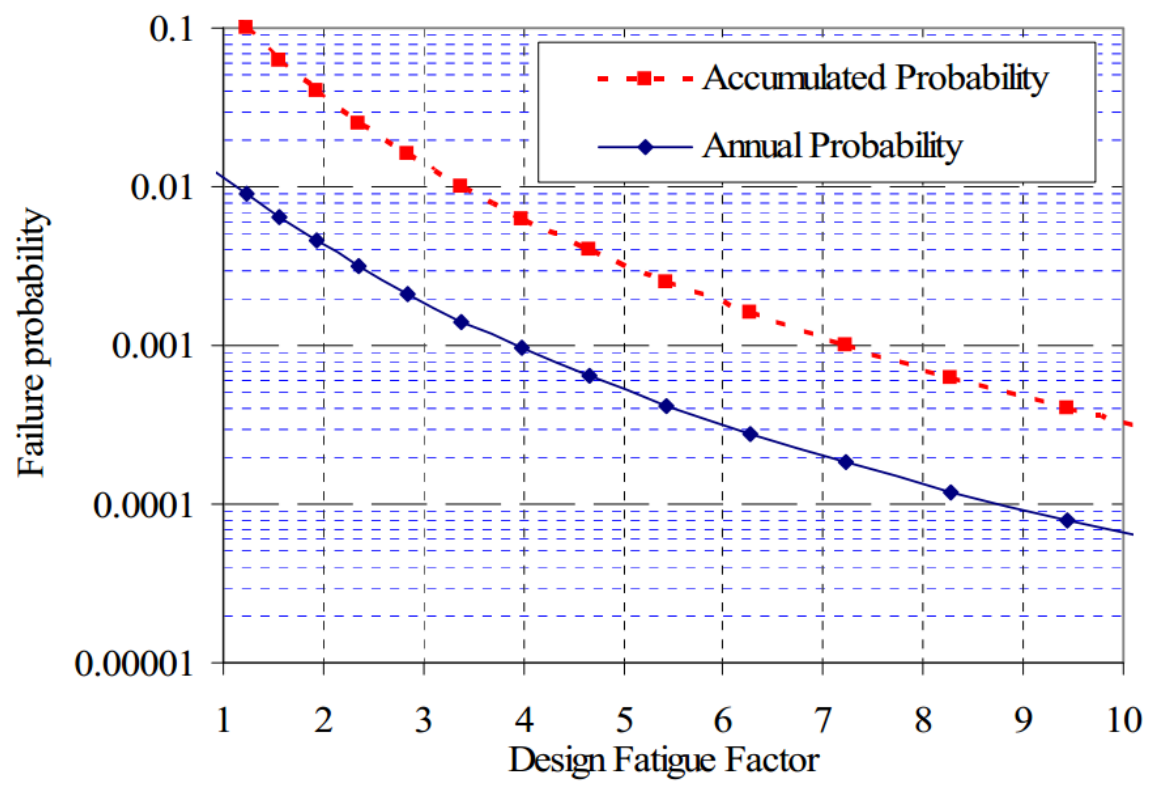


Figure 21: Effect of DFF on probability of failure (8).

To choose which DFF to use, DNV recommends that the DFF is dependent on the significance of the structural component with respect to structural integrity and availability for inspection and repairs. DFF should be applied to the calculated fatigue life, and should be longer than the designed fatigue life times DFF. Alternatively the cumulative damage times the DFF should be less than or equal to 1.

Table 3 shows DNV recommendations for suggestive use of DFF for a low consequence structural part that satisfies the accident limit state condition (16).

Table 3: Suggested DFF for low consequence structural part from DNV (16)

Table A1 Design fatigue factors (DFF)	
DFF	Structural element
1	Internal structure, accessible and not welded directly to the submerged part.
1	External structure, accessible for regular inspection and repair in dry and clean conditions.
2	Internal structure, accessible and welded directly to the submerged part.
2	External structure not accessible for inspection and repair in dry and clean conditions.
3	Non-accessible areas, areas not planned to be accessible for inspection and repair during operation.

4.12 Non Destructive Testing

All welds should be checked by NDT methods after welding, to ensure sufficient quality of the weld. Reference is made to standards for specific NDT methods. Table 4 shows DNVs recommendations for NDT methods of different weld types and joints (16). Acceptance level of flaws should be made after the same standard as the design was made of. For example if DNV design is used, DNVs acceptance level of flaws should be used.

Table 4 showing DNVs NDT recommendations (8)

Table B1 Minimum extent (in %) of non-destructive testing for structural welds						
Structural category	Inspection category	Type of connection	Test method			
			Visual	Magnetic ¹⁾	Radiography ²⁾	Ultrasonic ³⁾
Special / Essential	I	Butt weld	100%	100%	100%	-
		Cross- and T-joints, full penetration welds	100%	100%	-	100%
		Cross- and T-joints, partly penetration and fillet welds	100%	100%	-	-
Primary	II	Butt weld	100%	20% ⁴⁾	10%	-
		Cross- and T-joints, full penetration welds	100%	20%	-	20%
		Cross- and T-joints, partly penetration and fillet welds	100%	20%	-	-
Secondary	III	Butt weld	100%	Spot ⁵⁾	Spot ⁵⁾	-
		Cross- and T-joints, full penetration welds	100%	Spot ⁵⁾	-	Spot ⁵⁾
		Cross- and T-joints, partly penetration and fillet welds	100%	Spot ⁵⁾	-	-

1) Liquid penetrant testing to be adopted for non ferro-magnetic materials
2) May be partly or wholly replaced by ultrasonic testing upon agreement
3) Ultrasonic examination shall be carried out for plate thicknesses of 10 mm and above
4) For weld connections on hull shell not subjected to high residual stress, spot check will be accepted as sufficient.
5) Approximately 2 to 5%

Comments on the test methods (17):

Visual testing: detects surface flaws by for example looking at it or by the aid of computer controlled camera.

Magnetic testing: Iron particles are dusted to the surface of the part, and a magnetic field is introduced. Surface flaws and near surface flaws disrupt magnetic field and the iron particles gather above the flaw.

Radiography testing: “Photographs” of the part is taken by the use of X-rays or gamma-radiation. The resulting photograph on film, or other source, shows the flaws by different radiation strength depending on the thickness of the material. Since the detecting source is needed on the other side of the radiation source, both sides needs to be available.

Ultrasonic testing: High frequency sound waves are sent into the material, when the waves hit a flaw, it is reflected and sent back to a detector. The deflection time is measured and usually displayed by a wave-formed graph. The angel of the waves can be adjusted, so that the detector can be at the same side as the source.

4. 13 Fabrication time

Fabrication time and cost is mostly done by the fabricator to best estimate cost of the welding for market competition reasons (2). And most calculation models are based on this.

For design purposes it might be important to know right away if it is necessary to consider a fillet weld instead of butt weld. Since most fabricators give a price estimate on what the designer has designed. And fabricator might not know the reason why the specific welds are chosen.

According to one example with hollow sections with diameter of 200mm, there could be saved 55 min per hollow section by changing two full penetration welds with two fillet welds as shown in figure 22. (18).

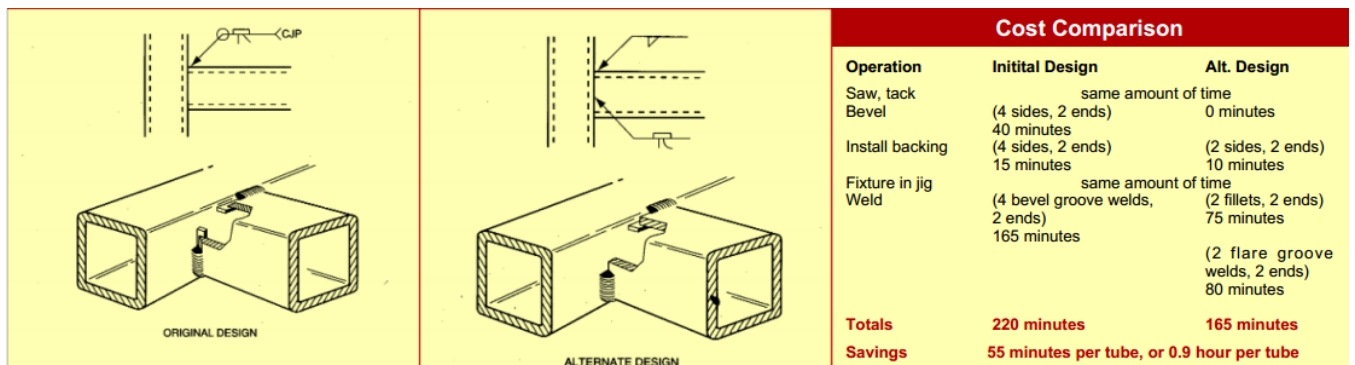


Figure 22: Cost estimation example for designer (18)

Assuming weld preparation time is the most time consuming difference between full penetration welds and fillet welds. This will be weighted here.

Following calculations are based on high speed acetylene cutting, although newer methods have been developed, like plasma and laser cutting, which have higher cutting speed.

For acetylene (high speed) cutting can be estimated by; cutting time per unit length t_c [min/m] (19):

Formula for cutting:

I, V, 1/2V butt welds 2-15 mm (19):

$$t_c = 0.9561 * K_r * t^{0.25}$$

X, K butt welds 10-40 mm (19):

$$t_c = 0.6911 * K_r * t^{0.3803}$$

t = thickness of plate to be cut

For partial penetration assuming thickness equal to vertical depth of fillet in plate.

K_r = complication factor for weld geometry with shape angle, $45^\circ = 1.45$, $30^\circ = 1.25$, $0^\circ = 1$ (19)

Formula for grinding preparation t_g [min/m] (19) :

$$t_g = \frac{l}{Q_i}$$

Where $Q_i = 750, 500, 375, 300$ [mm/min] is recommended for thickness 10, 20, 30 and 40 [mm] (19).

Simplified preparation time: $t_p = t_c + t_g$ [min/m]

Table 5 and graph in figure 24 showing cutting time, grinding time, preparation time in relation to thickness of the plate welded for I, V, 1/2V butt welds with thickness 2-15 mm: Kr is set to 1.25

Table 5: Cutting-, grinding- and preparation time for $2 \leq t \leq 15$ for I, V, 1/2 V butt welds

Thickness t [mm]	Cutting time: t_c [min/m]	Grinding time: t_g [min/m]	Preparation time: t_p [min/m]
2	1.42	1.33	2.75
3	1.57	1.33	2.91
4	1.69	1.33	3.02
5	1.79	1.33	3.12
6	1.87	1.33	3.20
7	1.94	1.33	3.28
8	2.01	1.33	3.34
9	2.07	1.33	3.40
10	2.13	1.33	3.46
11	2.18	2.00	4.18
12	2.22	2.00	4.22
13	2.27	2.00	4.27
14	2.31	2.00	4.31
15	2.35	2.00	4.35

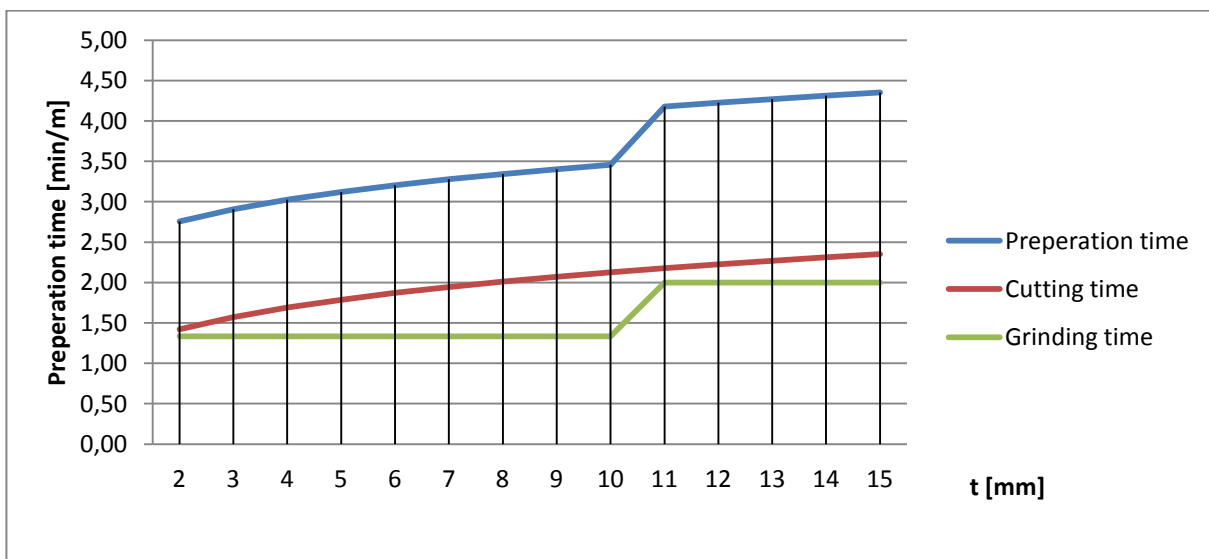


Figure 23: Cutting-, grinding- and preparation time for $2 \leq t \leq 15$ for I, V, 1/2 V butt welds (note 0,50 = 0.50 etc)

Table 6 and graph in figure 25 showing cutting time, grinding time, preparation time in relation to thickness of the plate welded for X, K butt welds with thickness 10-40 mm: Kr is set to 1.45

Table 6 Cutting-, grinding- and preparation time for $10 \leq t \leq 40$ for X and K butt welds

Thickness	Cutting time:	Grinding time:	Preperation time:
t [mm]	t_c [min/m]	t_g [min/m]	t_p [min/m]
10	2.41	1.33	3.74
11	2.49	2.00	4.49
12	2.58	2.00	4.58
13	2.66	2.00	4.66
14	2.73	2.00	4.73
15	2.81	2.00	4.81
16	2.88	2.00	4.88
17	2.94	2.00	4.94
18	3.01	2.00	5.01
19	3.07	2.00	5.07
20	3.13	2.00	5.13
21	3.19	2.67	5.86
22	3.25	2.67	5.91
23	3.30	2.67	5.97
24	3.36	2.67	6.02
25	3.41	2.67	6.08
26	3.46	2.67	6.13
27	3.51	2.67	6.18
28	3.56	2.67	6.23
29	3.61	2.67	6.27
30	3.65	2.67	6.32
31	3.70	3.33	7.03
32	3.74	3.33	7.08
33	3.79	3.33	7.12
34	3.83	3.33	7.16
35	3.87	3.33	7.21
36	3.92	3.33	7.25
37	3.96	3.33	7.29
38	4.00	3.33	7.33
39	4.04	3.33	7.37
40	4.08	3.33	7.41

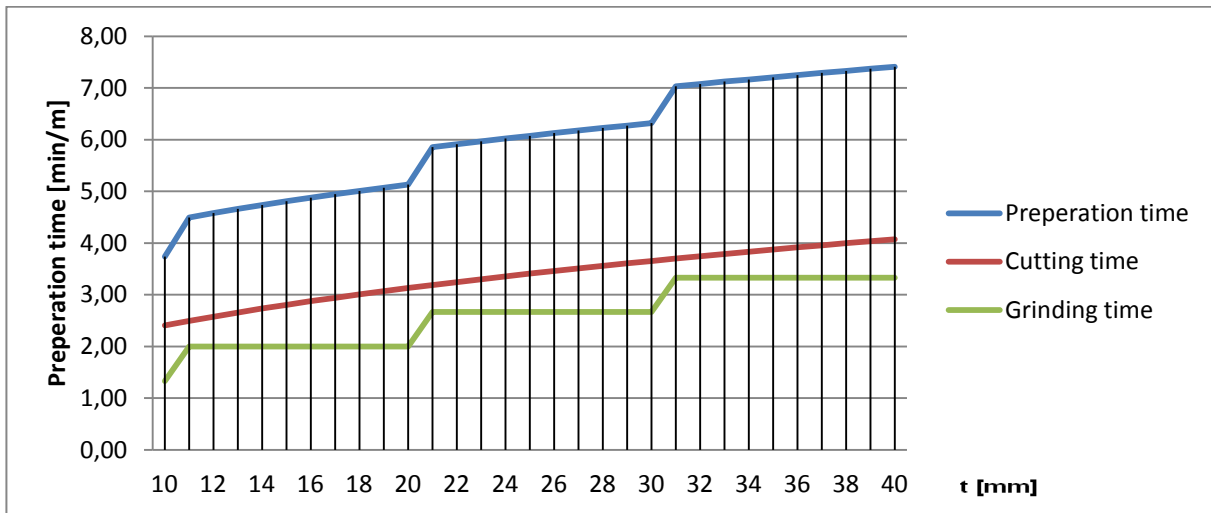


Figure 24: Cutting-, grinding- and preparation time for $10 \leq t \leq 40$ for X and K butt welds (note 1,00 = 1.00 etc)

5.0 Description of example

The goal is to check optional solutions for a weld detail, shown in figure 26, in a traverse beam in a work over unit derrick's hoisting system. The location of the weld detail is shown in figure 27. Thickness of the plates under tensile load is 30 mm and thickness of the stiffener is 40 mm.

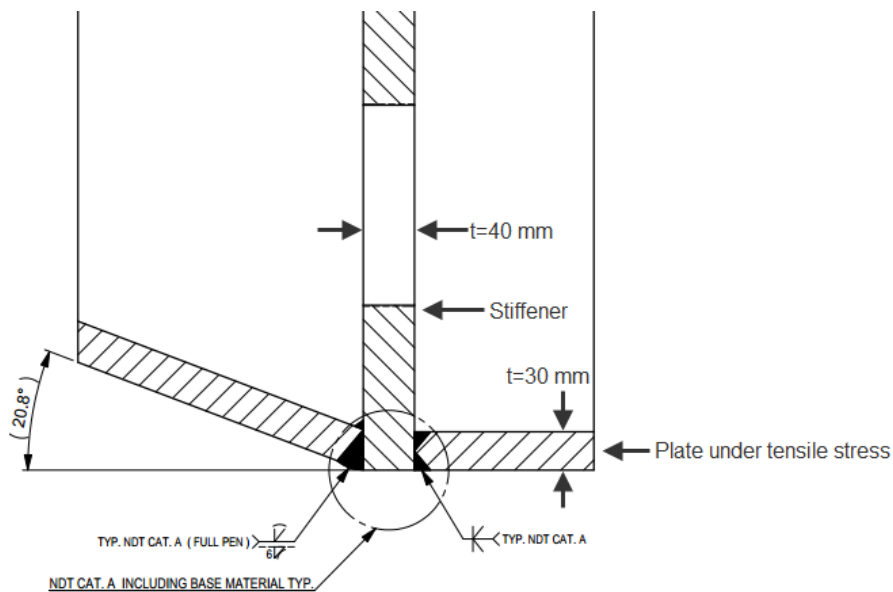


Figure 25: Cut out cross-section of weld detail

The stiffener is also part of the load bracket, distributing the force in the beam, shown in figure 27

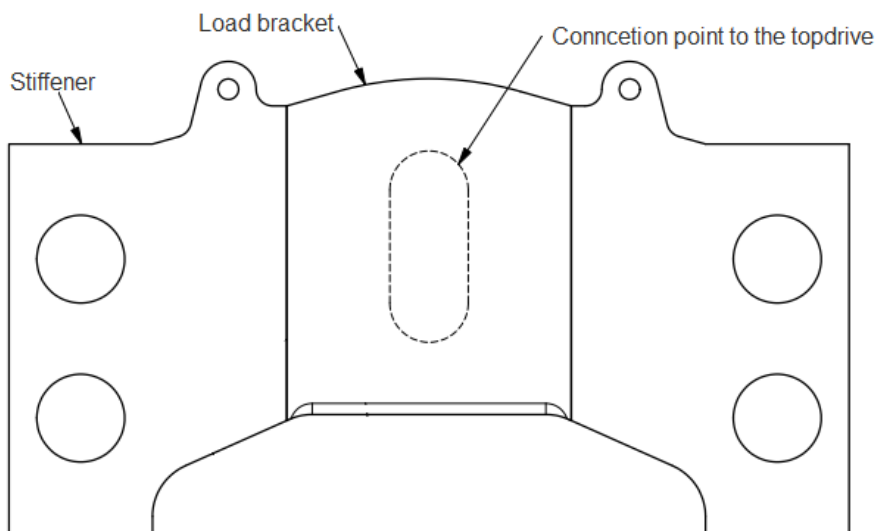


Figure 26: Stiffeners connected to one of the load brackets

The load that needs to be handled is the weight of the pipes which is set together one by one. For each time a new pipe is connected the load is reset to self weight of the beam, and the next amplitude will increase with the weight of one pipe. Therefore the load amplitude is linearly increased for each pipe at setup, and linearly decreased at demounting. The number of cycles

for each down hole trip is 1 454, and is designed to be used 300 times. Which make a total of 436 200 cycles, or approximately $5 \cdot 10^5$ cycles. The load data is collected from an external and internal report on load history. The beam is supported by four flexible connections and the load is transferred by the top drive through the traverse beam shown in figure 28 and 29. The traverse beam is made by welding plates together, making up several boxes to a 3D uniform beam, as shown in figure 28.

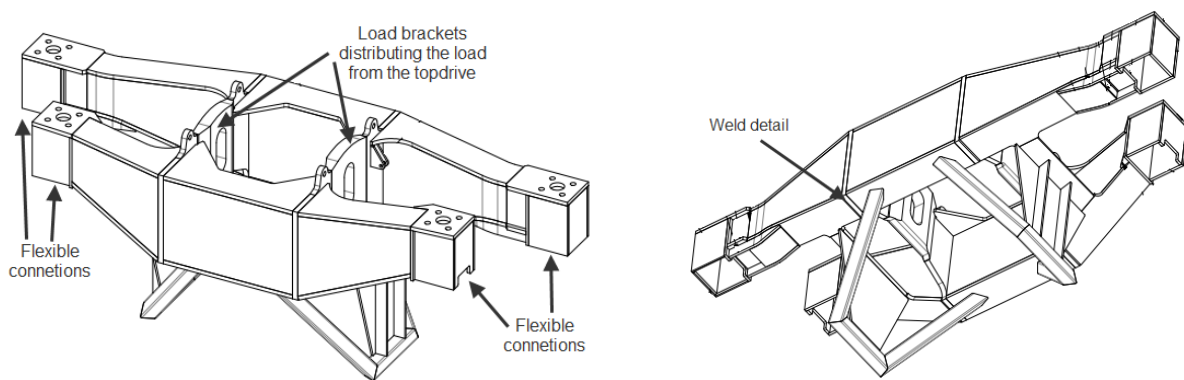


Figure 27: 3D beam with the load points, location of weld detail and graphical display of the plates welded together

The two stiffeners in each beam, for inspection reason, make the top and bottom plates discontinues. There is question if this makes the welding more complicated and therefore more time consuming and expensive. There is also doubt if the total strength of the beam will suffer from these discontinuities.

The load history and boundary conditions are collected from the original design calculation report. The boundary conditions and where the loads are applied are seen in figure 29. The load used in the stress calculations are without any factors. For fatigue calculations DFF is applied to D after DNV recommendations for risk assessment.

The pull load (P) and drilling torque (T) is transferred from the top drive through the load brackets (figure 27) into the transverse beam seen in figure 28.

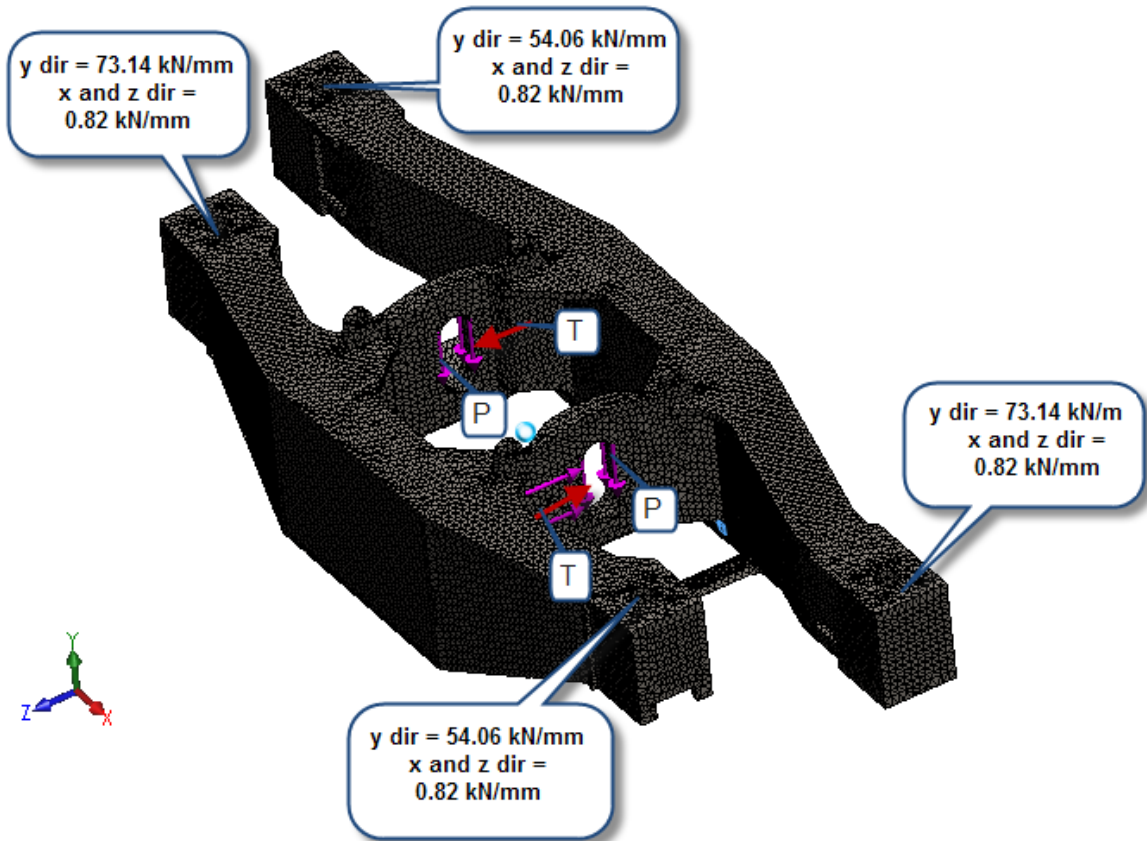


Figure 28: Meshed model in Solidworks with boundary conditions and loads

The different weld designs that were checked are shown in figure 30 and given number categories for easier notation later in the thesis, from the top left; 1, 2, 3, from bottom left; 4, 5, 6. Weld 1 is the original design with a 45° weld with a = 6 on the top of the left plate. Weld 2 is designed with butt-welded stiffener onto the bottom plate with 0° transition. Weld 3 is designed with K butt weld onto the bottom plate, with 45° transition. Weld 4 is designed with a butt weld onto the bottom plate with 30° transition. Weld 5 is a fillet weld onto the bottom plate with leg lengths = 30. Weld 6 is a partial penetrating weld with leg lengths = 20 mm. Weld 5 and 6 is designed open on the side of the load bracket and closed in by a plate on the other side, see Appendix D figure D.2. They are also assumed to be almost non-load-carrying since the stiffener is welded together with plates in the beam at three more places, the load is also compressive.

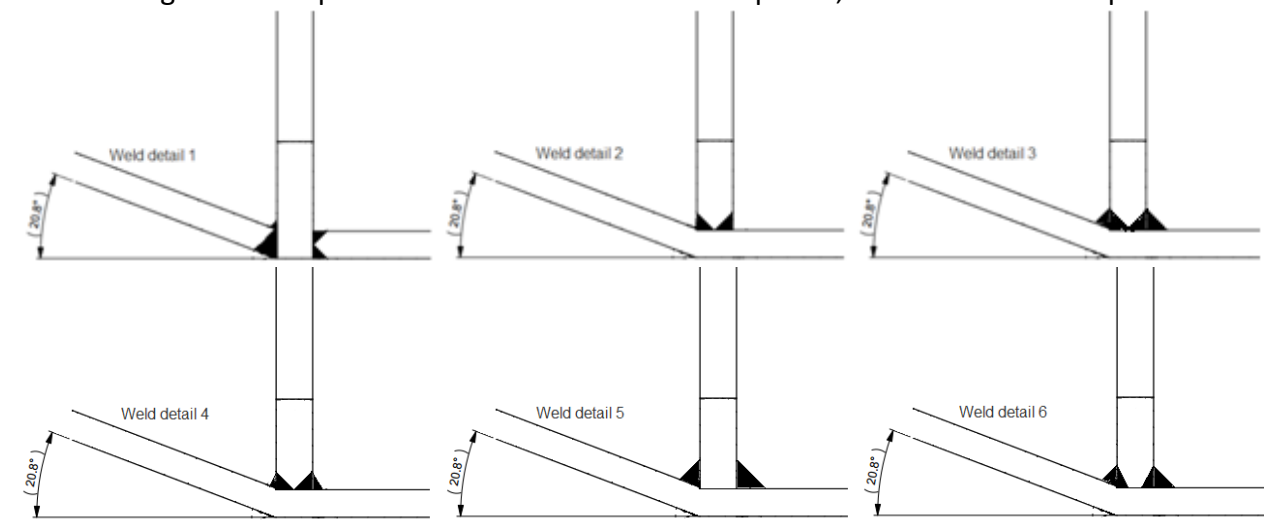


Figure 29: The different weld designs with number categories

The original calculation report have concluded that the beam is sufficiently strong according to Ec3 and API 8C for the different limit states, and is assumed to be correct.

There were done hand calculations in the original report to check if results from the simulation were reliable and was found to be so.

5.1 Load history for each down-hole operation:

The method and formulas are collected from an internal load history report for rack and pinion drive.

Length of pipe

$$L_p := 13.72\text{m}$$

Weight pipe

$$W_p := 40 \frac{\text{kg}}{\text{m}} \cdot L_p = 548.8\text{kg}$$

Number of pipe joins at depth 5000m:

$$n_{p,5000\text{m}} := \text{round}\left(\frac{5000\text{m}}{L_p}\right) = 364$$

Number of travels $i=0,1,2,\dots, n_{p,\text{max}}$ from joints full trip i.e. down hole:

$$n_{p,\text{max}} := 2 \cdot n_{p,5000\text{m}} - 1 = 727$$

$$i := 0, 1 \dots 2 \cdot n_{p,\text{max}} + 1$$

Function helping to defining load function (step function):

$$\text{on}(i) := \left| \sin\left(\frac{i\pi}{2}\right) \right|$$

Additional functions for load history definition:

$$x(i) := \begin{cases} 1 & \text{if } 3 \leq i \leq n_{p,\text{max}} \\ 0 & \text{otherwise} \end{cases}$$

$$y(i) := \begin{cases} 1 & \text{if } n_{p,\text{max}} + 1 \leq i \leq 2 \cdot n_{p,\text{max}} \\ 0 & \text{otherwise} \end{cases}$$

$$z(i) := \begin{cases} 1 & \text{if } 0 \leq i < 3 \\ 1 & \text{if } 2 \cdot n_{p,\text{max}} < i \leq 1455 \\ 0 & \text{otherwise} \end{cases}$$

Weight of top drive

$$W_{\text{topdrive}} := 8000\text{kg}$$

Weight of traverse beam (linear distributed)

$$W_{\text{traverse}} := 3000\text{kg}$$

Load function $F_u(i)$ describes the load that has to be held by the traverse beam, graphicly displayed in figure 31 and 32.

$$F_u(i) := \left[\left[\left(\frac{i-1}{2} \right) \cdot W_p \cdot \text{on}(i) + (W_{\text{topdrive}} + W_{\text{traverse}} + W_p) \right] \cdot x(i) \dots \right. \\ \left. + \left[\left(\frac{2 \cdot n_{p.\text{max}} - i}{2} \right) \cdot W_p \cdot \text{on}(i+1) + (W_{\text{topdrive}} + W_{\text{traverse}} + W_p) \right] \cdot y(i) \dots \right. \\ \left. + (W_{\text{topdrive}} + W_{\text{traverse}} + W_p) \cdot z(i) \right]$$

$$F_u(n_{p.\text{max}}) = 2.11 \times 10^5 \cdot \text{kg}$$

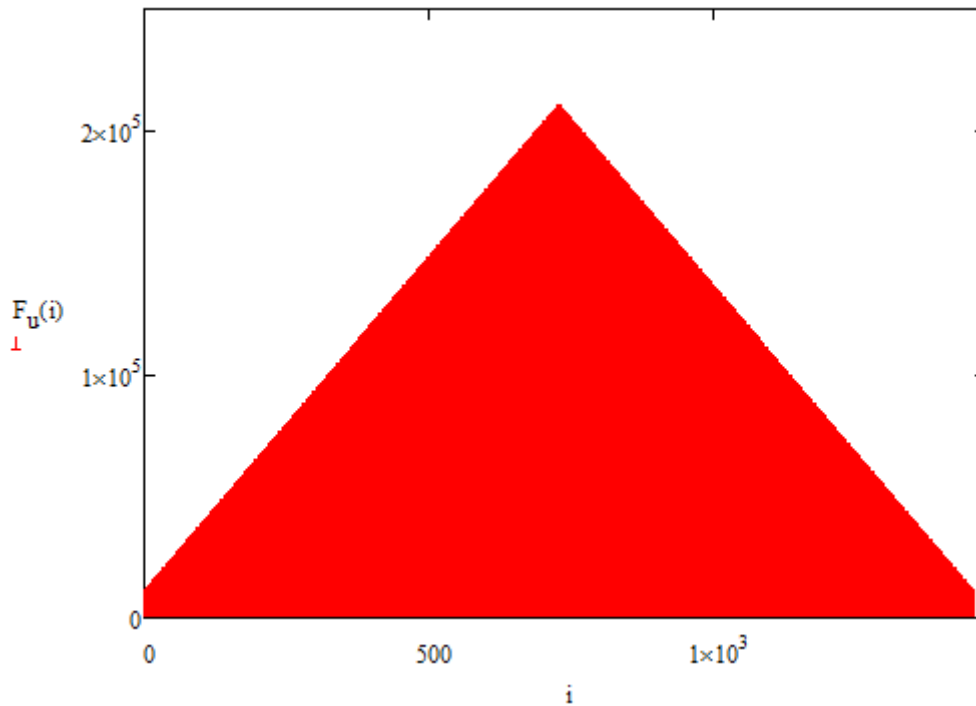


Figure 30: Load history, $F_u(i)$ [kg] for 1454 cycles (i)

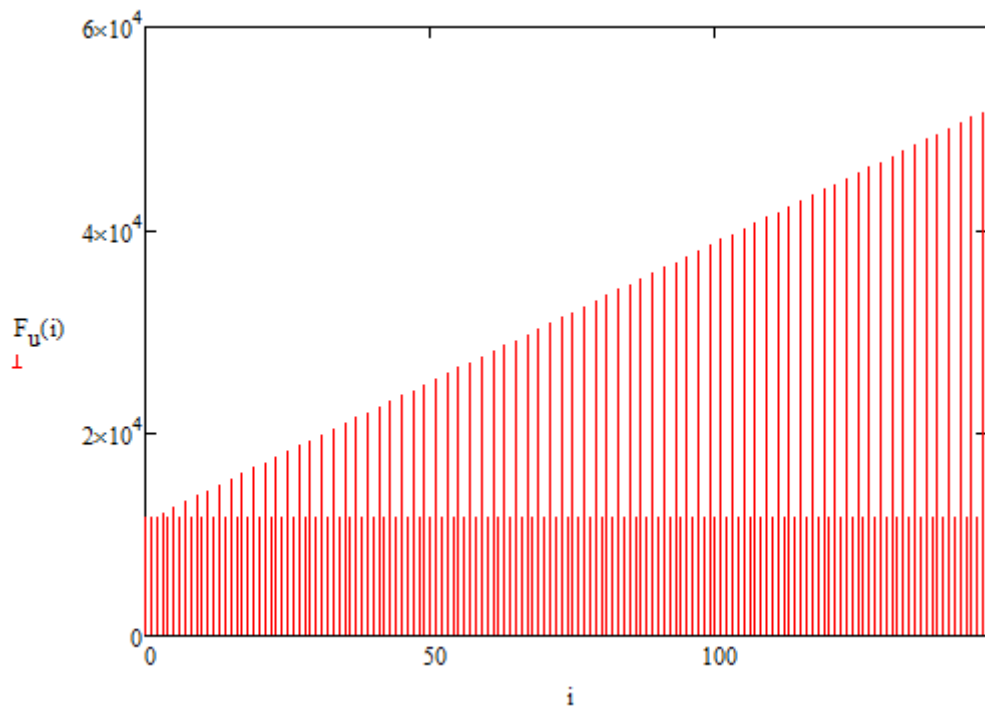


Figure 31: Showing each load for $F_u(i)$ [kg] for the first 150 cycles (i)

5.2 Description of Solidworks

The following chapter is based on information from the Solidworks help function.

Solidworks is a 3D CAD program for easy design of mechanical parts and structures. With the “simulation” add-in it can also be used for quite accurate engineering analysis with the use of finite element method (FEM). (20)

The calculations in Solidworks are based on the assumption of Linear-static analysis.

When given a meshed model with boundary conditions and loads, the linear-static analysis program calculation proceeds with constructing and solving a system of linear simultaneous finite element equilibrium equations to calculate the displacement components at each node. From the displacement the strain is calculated, and from the stress-strain relationship the stresses are calculated. The order of calculation graphically displayed in figure 33 (20).

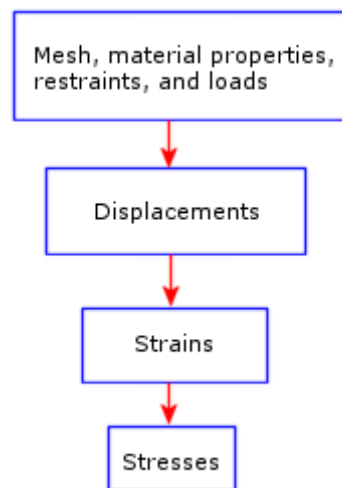


Figure 32: Illustrating the order of calculation (20)

For optimal results the stress results are first calculated at Gaussian points, points located inside each element. Then the program calculates the nodal stress of each element by extrapolating the results available at the Gaussian points.

Since finite element method is an approximation method, the stress results viewed is an average for each node for corresponding element (element stress), or average of element stress sharing a node (nodal stress).

The transverse beam is a 3D model, therefore solid elements are used. Solidworks operates with tetrahedral solid elements, and for most accurate results parabolic elements are used, hooking of the “High quality mesh” option. Each node in a solid element has three degrees of freedom that represent the translation in three orthogonal directions (20). Solidworks uses X, Y, and Z directions of the global Cartesian coordinate system in formulating the problem (20).

A parabolic tetrahedral element is defined by four corner nodes, six mid-side nodes, and six edges, shown in figure 34 (20).

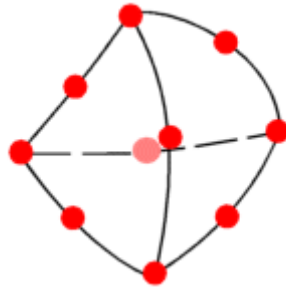


Figure 33: Parabolic tetrahedral element with 10 nodes shown as red dots (20)

With the same number of elements, parabolic elements usually give better results than linear elements (20). This is because they represent curved boundaries better and produce better mathematical approximations (20). However, the parabolic elements require more computer power.

5.3 Modeling for Hot-spot:

Since Solidworks uses 10 node elements, element size of $0.5t$ and two layers of elements in the thickness direction are suggested near the weld. Mesh size of 30mm was used as general mesh size, and a mesh size of 15mm ($0.5t$) was used from 100mm near the weld to ensure smooth transition. There were modeled in lines at the distances $0.5t$ and $1.5t$ for ensuring node points at these locations and extrapolating maximum principal stress at the intersection line. This was done by using “surface extrude”-tool at the distances 100 mm from the stiffener, $1.5t$ and $0.5t$ from the weld toe, the horizontal distance was set to 130 mm, 100mm and 60mm. Then using the “split”-tool giving three different bodies, “delete body”-tool was used to delete the surface extruded. Figure 35 showing extrapolation lines at $0.5t$ and $1.5t$ distances from the weld toe and the change in mesh size near the weld.

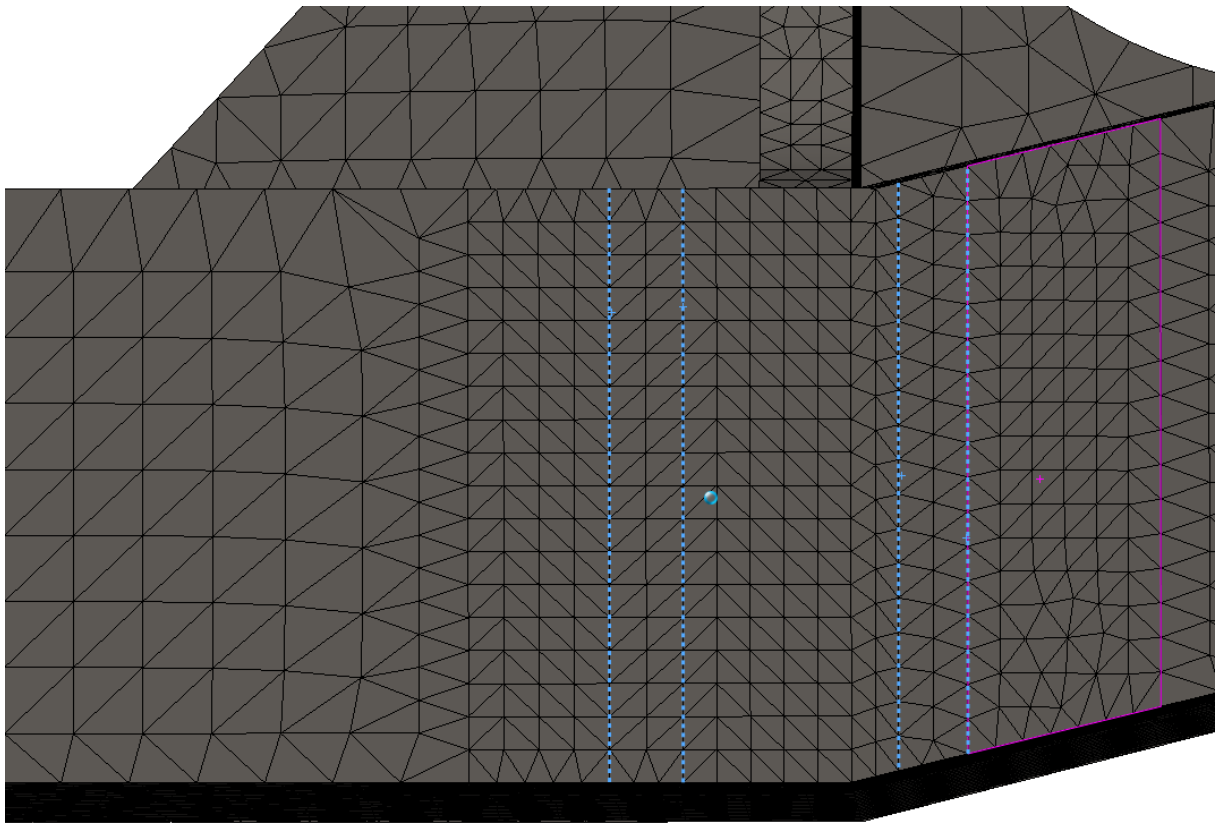


Figure 34: Extrapolation lines at distances $0.5t$ (inner lines) and $1.5t$ (outer lines) from the weld toe

When meshing, the “control mesh”-tool was used, the split bodies were selected and mesh size was set to 15mm. The “component contact”-tool was used so all the bodies were counted as a uniform structure. Material property was set to “Steel AISI 1020”, giving properties shown in table 7:

Table 7: Material properties of AISI 1020-steel in Solidworks

Property	Value	Units
Poissons Ratio	0.29	N/A
Shear Modulus	$7.7e+010$	N/m^2
Density	7900	kg/m^3
Tensile Strength	420507000	N/m^2
Compressive Strength in X		N/m^2
Yield Strength	351571000	N/m^2
Thermal Expansion Coefficient	$1.5e-005$	$/K$
Thermal Conductivity	47	$W/(m \cdot K)$
Specific Heat	420	$J/(kg \cdot K)$

Although steel with $f_y = 420$ MPa was used in the beam, since the analysis is linear-elastic, it is assumed to give correct results.

5.4 Modeling for notch-stress:

An effective notch radius of 1 mm was modeled and a volume around notch is model as a tube with radius 2 mm, the mesh size of the notch and volume is set to 0.25mm (1/4 of notch radius ref IIW) ensuring at least 3 layers of unrefined meshing. There was used a mesh size of 0.3mm at first which, according to DNV, were sufficient for the 4 elements for a quarter of a circle criteria. But this gave lower stress results, reference appendix H figure H. 2. Lower radius of the volume around the notch was also tested, but these often gave unwanted mesh geometry and errors which may have originated from the mesh geometry, reference appendix H figure H.1.

Further a 10 mm² squared column around the notch with element size of 1 mm.

For partial penetrating welds, there was modeled a U shaped root instead of the key-hole model recommended in DNV and IIW. This was done to the decrease the modeling and meshing time.

This is assumed to give conservative results according to an IIW report on notch-stress meshing (13). Figure 36 showing U-shaped notch with radius of 1 mm, volume around the notch with unaltered mesh and mesh size from 0.25 mm to 1 mm.

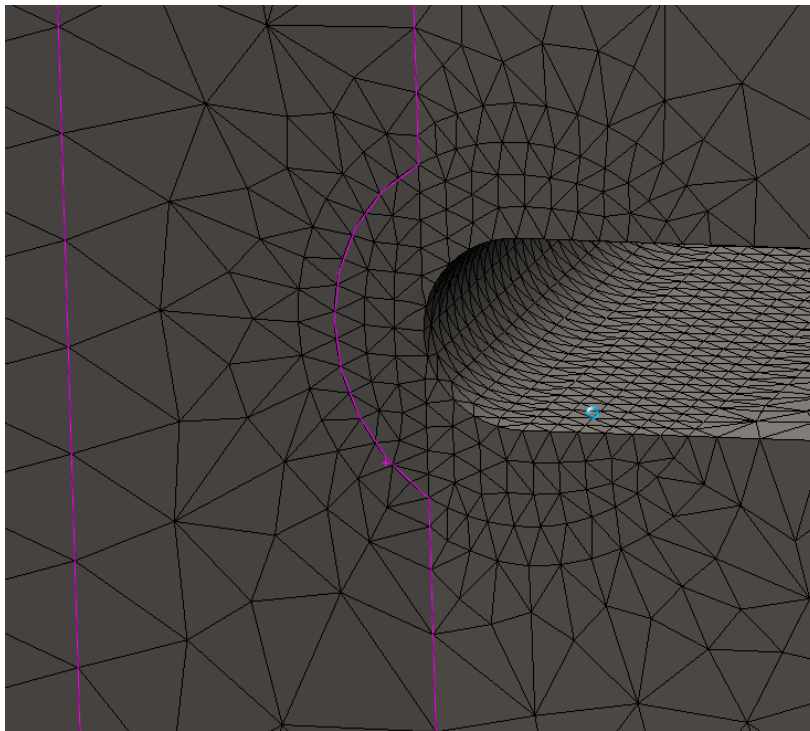


Figure 35: Screenshot of mesh geometry from FEA model in Solidworks, U-shaped hole with radius of 1 mm, unaltered mesh with mesh size 0.25 mm and transition from 0.25 mm mesh size to 1 mm mesh size.

Then two more boxes with element size 5mm and 15mm to ensure the change in mesh size is not to drastic (8).

The notch is modeled with the “fillet” tool. The volumes with different mesh size were made by “surface extrude”-tool similar to the modeling in the hot-spot method. It should be noted that the different volumes were made all the way through the structure detail to ensure proper mesh geometry.

The time used for the extra modeling and solving time was approximately 40 min, +-10 min. To check if the mesh modeling was correct, a reference model was made according to DNV, and was found to be so, see Appendix E. (8)

To decreasing mesh and solving time for all cases, the weld toe and root with maximum stress were found by using a mesh size of 0.5mm at the notch, and mesh size of 5mm in the volume around. The mesh geometry was restricted by 1.5 l/b ratio and assumed to give good enough results. Figure 37 showing meshing and Figure 38 showing the density of nodes which have a higher value than 300 MPa of 1st principal stress.

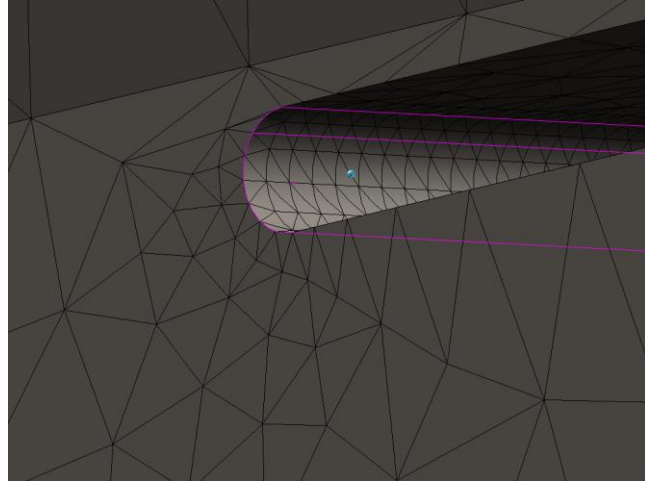


Figure 36: Mesh geometry, 0.5 at the notch surface and transition to 5 mm mesh, for finding the root/toe with maximum stress

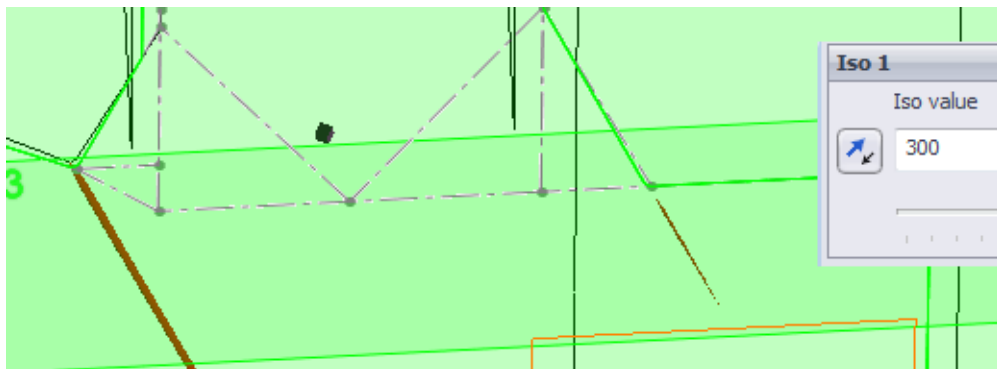


Figure 37: Stress density at weld toes for 1st principle stress from 300 MPa and up

5.6 Fatigue damage calculation

The fatigue damage calculation was made according to the Palmgren-miner rule and S-N curves after calculation from Ec3. Since the number of cycles are $5 \cdot 10^5$, less than $5 \cdot 10^6$, this is assumed to give correct results (8).

The following procedure was used:

$$\Delta\sigma_c := 225\text{MPa}$$

$$N_c := 2 \cdot 10^6$$

Constant amplitude fatigue limit $\Delta\sigma_D$ according to section 7.1 Ec3

$$\Delta\sigma_D := \left(\frac{2}{5}\right)^{\frac{1}{3}} \cdot \Delta\sigma_c = 165.781\text{-MPa} \quad N_D := 5 \cdot 10^6$$

Cut off limit $\Delta\sigma_L$ according to section 7.1 Ec3

$$\Delta\sigma_L := \left(\frac{5}{100}\right)^{\frac{1}{5}} \cdot \Delta\sigma_D = 91.06\text{-MPa} \quad N_L := 10^8$$

$$m_1 := \frac{\log\left(\frac{\Delta\sigma_D}{\Delta\sigma_c}\right)}{\log\left(\frac{N_D}{N_c}\right)} = -0.333$$

$$m_2 := \frac{\log\left(\frac{\Delta\sigma_L}{\Delta\sigma_D}\right)}{\log\left(\frac{N_L}{N_D}\right)} = -0.2$$

The function $N(\Delta\sigma_R)$ is created. $N(\Delta\sigma_R)$ calculates endurance limit based on 7.1 Ec3

$$N(\Delta\sigma_R) := \begin{cases} N_D \cdot \left(\frac{\Delta\sigma_R}{\Delta\sigma_D}\right)^{\frac{1}{m_1}} & \text{if } \Delta\sigma_R \geq \Delta\sigma_D \\ N_L \cdot \left(\frac{\Delta\sigma_R}{\Delta\sigma_L}\right)^{\frac{1}{m_2}} & \text{if } \Delta\sigma_D > \Delta\sigma_R \geq \Delta\sigma_L \\ \infty & \text{if } \Delta\sigma_R < \Delta\sigma_L \end{cases}$$

Some selected values for $N(\Delta\sigma_R)$ are tested and referenced with figure 39

$$N(\Delta\sigma_C) = 2 \times 10^6$$

$$N(\Delta\sigma_L) = 1 \times 10^8$$

$$N(\Delta\sigma_D) = 5 \times 10^6$$

$$N(200\text{MPa}) = 1.823 \times 10^5$$

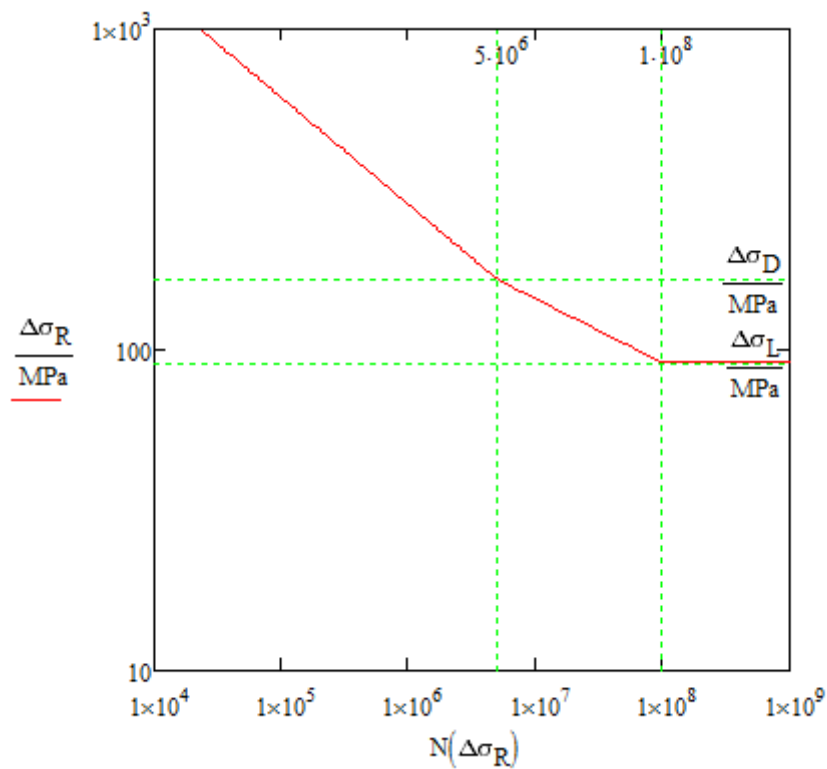


Figure 38: Corresponding S-N curve for $\Delta\sigma_c$ (calculated)

Maximum stress amplitude

$$\Delta\sigma_{\max} := \sigma_{\text{eff}} \cdot \frac{F_u(n_{p.\max}) - F_u(1)}{F_u(n_{p.\max})} = 411.92 \cdot \text{MPa}$$

Calculation of fatigue life according to damage summation:

$$N(i) := \text{round} \left[N \left[\frac{F_u(i)}{F_u(n_{p.\max})} \cdot (\gamma_{\text{FF}} \cdot \Delta\sigma_{\max}) \right] \right]$$

Number of times direct stress load (i) is experienced for trough life (reference internal load history):

$$n_i := 300$$

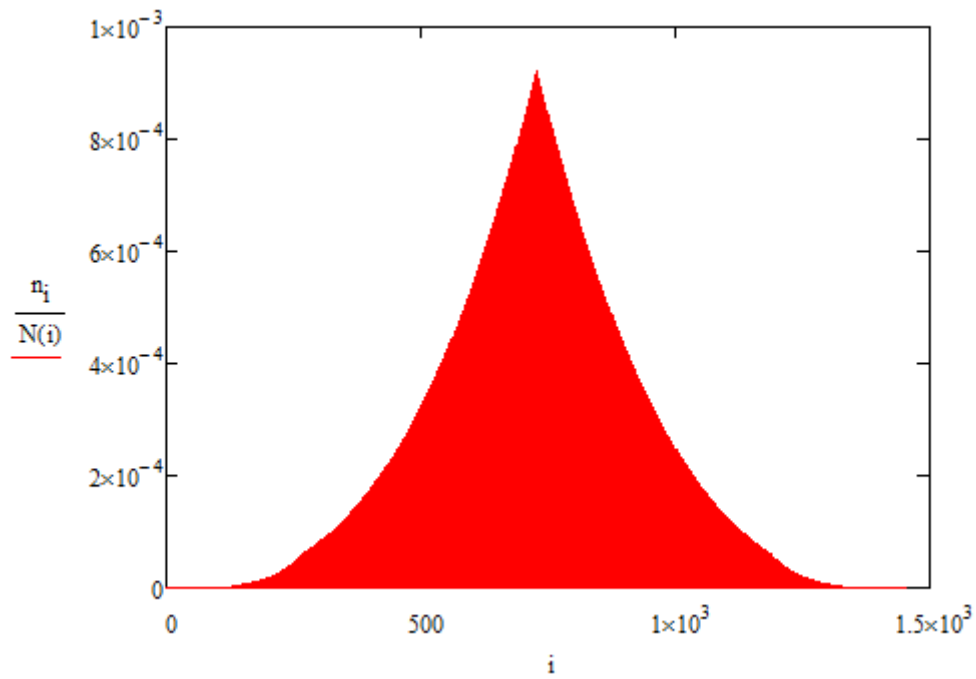


Figure 39: Total fatigue damage accumulated is area “under the curve”

$$D := \sum_{i=1}^{2n_{p.\max}+1} \frac{n_i}{N(i)}$$

D = 0.18

Note: By changing the factors for $\Delta\sigma_D$ and $\Delta\sigma_L$, to $\left(\frac{1}{5}\right)^{\frac{1}{3}}$ for $\Delta\sigma_D$ and $\left(\frac{1}{10}\right)^{\frac{1}{5}}$ for $\Delta\sigma_L$, interpolating the constant amplitude limit to 10^7 , the same procedure can be used for DNV and IIW recommendations.

5.7 Risk analysis

The consequence of the beam failing could be severe, oil and gas pollution and the loss of human lives could be a reality. Therefore the probability of failure should be low. If designed with a weld which is unavailable for in-service inspection, the probability of failure should be even lower. Since the in-service inspection decreases the probability of failure by checking for possibility for a crack to grow large enough to increase probability of failure (8).

Because of the uncertainties in the calculation of fatigue damage and strength, to lower the probability, a DFF of 3 is suggested for a design with welds available for inspection.

For welds unavailable for inspection, DFF of 10 is recommended (16). Suggestive DFF factors are shown in table 8.

Because of the high risk environment, to avoid crack start from the weld root, which might not be detected (1) fillet welds and partial penetration welds designs should be carefully checked.

Table 8: Suggested DFF for high to low consequence environment to decrease risk

Consequence	Damage Fatigue Factor		Achieved probability	Achieved Risk
	Available for inspection	Unavailable for inspection		
High	3	10	Low	Low
Medium	2	6	Low	Low
Low	1	3	Low	Low

6.0 Results:

According to the simulation study the maximum stresses in the specific welded area where attained when the torque was equal to zero, reference to figures G.5 in appendix G, therefore neglected in the fatigue study.

6.1 Hot-spot results:

The stresses were checked for the original design, butt welds with 0°, 45° and 30° transition (weld detail 1, 2, 3 and 4). The methods in DNV were used, method a) interpolation from lines 1.5t to 0.5t. Equation (8) for σ_{eff} method a;

$$\sigma_{eff} = \max \begin{cases} \sqrt{\Delta\sigma_{\perp}^2 + 0.81\Delta\tau_{//}^2} \\ \alpha|\Delta\sigma_1| \\ \alpha|\Delta\sigma_2| \end{cases}$$

Where $\Delta\sigma_{1/2}$ etc represents hot-spot stress.

For method b) $\Delta\sigma_{1/2}$ is multiplied by a factor of 1.12 for stress at 0.5t instead of interpolation. Equation (8) for σ_{eff} method b;

$$\sigma_{eff} = \max \begin{cases} 1.12\sqrt{(\Delta\sigma_{\perp})^2 + 0.81\Delta\tau_{//}^2} \\ 1.12\alpha|\Delta\sigma_1| \\ 1.12\alpha|\Delta\sigma_2| \end{cases}$$

Where $\Delta\sigma_{1/2}$ etc represents extrapolated stresses at 0.5t

The α factor in these equations are used if the stresses are parallel (to some degree) to the weld (8).

The simulation study was run and maximum stress was found at distances of 0.5t and 1.5t from the weld toe by selecting the lines with the “list selected”-tool, shown in figure 41. The tool lists all stresses at the line, and stress properties like maximum stress. In all cases the maximum 1st principal stress was highest, see Appendix F.

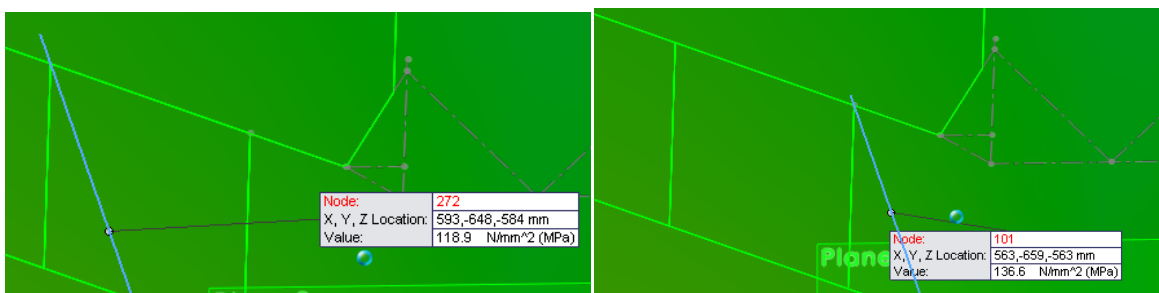


Figure 40: Maximum 1st principle stress at intersection lines at 1.5t and 0.5t for butt weld with 30° transition

When selecting the maximum stresses from both lines it is assumed to give a non-conservative results, as the interpolation line will be less steep, although the magnitude of the different stresses at the same area was below 1 %. The FAT 90 curve was used, since the stress extrapolation is according to DNV. For comparison reason, misalignment factor was neglected for the original design, would give an increase in stress by 10% (9). The results, represented in table 9, where almost the same. Method b) gave slightly higher results.

Table 9: Summarized results from the hot-spot method

Method:		a)			
Weld detail		1	2	3	4
Stress type					
σ_1 at 1.5t [MPa]		118.9	118.6	120.3	119.4
σ_1 at 0.5t [MPa]		136.6	136.8	136.8	136.8
σ_{eff} [MPa]		145.4	145.9	145.0	145.5
D		0.1	0.1	0.1	0.1
D*(DFF=10)		1	1	1	1
Method:		b)			
σ_{eff} [MPa]		153.0	153.2	153.2	153.2
D		0.12	0.12	0,2	0.12

6.2 Notch-stress results

The toe stresses were checked for original design, butt welds with 0°, 45° and 30° transition (weld detail 1, 2, 3 and 4) and the root stress for fillet weld and partial penetration (weld detail 5 and 6). The simulation study was run and maximum stress was found by the “list select”-tool and selecting the notch, shown in figure 42. For all cases 1st principle stress was the maximum stress, see Appendix F. For comparison reason, misalignment factor was neglected for the original design, would give an increase in stress by 10% (9).

Only the root stresses were checked for fillet and partial penetration, because of the reduced stiffness it is assumed that the toe stresses would be slightly higher than weld detail 2.

The maximum principal stress was used with the FAT225 SN curve after IIW recommendations (9). Results are summarized in table 10.

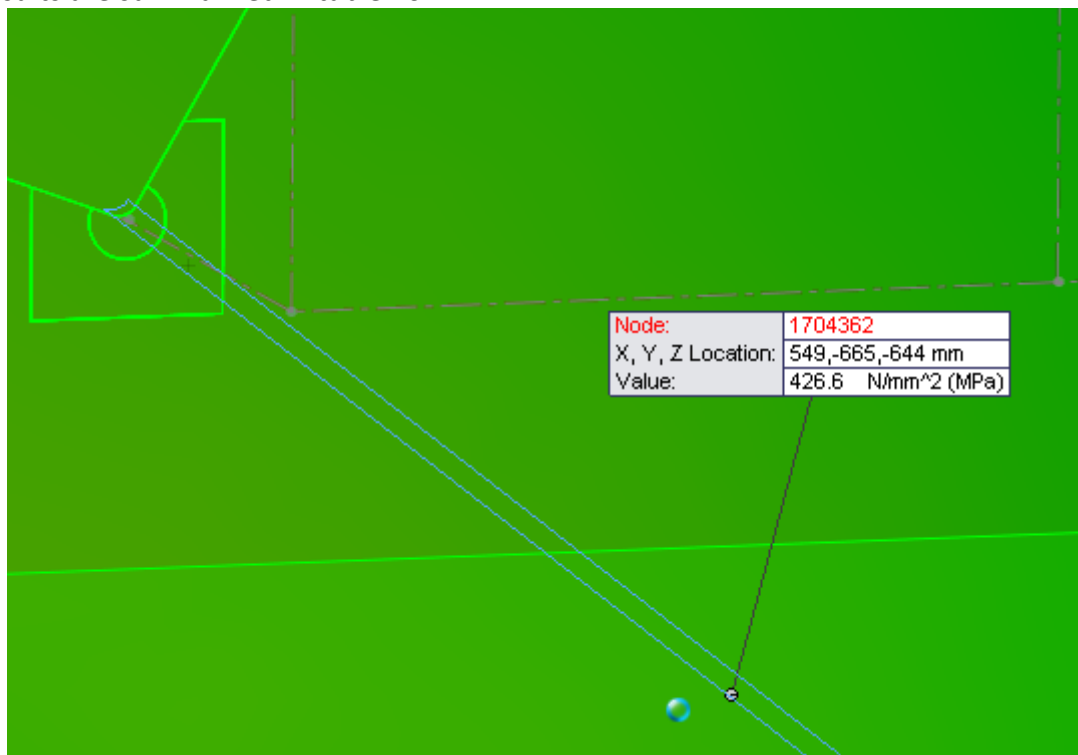


Figure 41: Extrapolation of maximum 1st principle stress at notch-surface

Table 10: Summarized results from notch-stress method

Weld detail	1	2	3	4	5	6
σ_n [Mpa]	426.6	415.7	462.9	435.8	380.4	285.0
D	0.16	0.15	0.21	0,18	0,12	0,05
D*(DFF=10)	1.6	1.5	2.1	1.8	1.2	0.5
D*(DFF=2)	0.32	0.3	0.42	0.36	0.24	0.1

6.3 Estimating preparation time:

The preparation time was estimated for the original design, new full penetration design and partial penetration design. For fillet weld design, preparation is not needed.

Original design:

16 different plates with thickness of 30 mm and length of 250 mm had to be cut and grinded

New full penetration designs:

4 different plates with thickness of 40 mm and length of 250 mm - 15 mm had to be cut

Partial penetration design:

4 different plates with thickness of 20 mm, assumed to be half of plate thickness, and length of 250 mm - 15 mm had to be cut

For fillet weld design: No preparation needed.

Simplified preparation time formula:

$$t_p = t_c + t_g = 0.6911 * K_r * t^{0.3803} + \frac{l}{Q_i}$$

$K_r = 1.45$ and $Q_i = 500\text{mm}/\text{min}$ for partial

$Q_i = 375\text{mm}/\text{min}$ for original

$Q_i = 300\text{mm}/\text{min}$ for full

The results showed that there is not much time to be saved from weld preparation when the number of plates that have to be prepared is small. Table 11 shows the time used for cutting, grinding, preparation and the time saved accordingly to the original design.

Table 11: Cutting-, grinding-, preparation time and timed saved

Type	t_c [min]	t_g [min]	t_p [min]	Time saved [min]
Original	14.61	1.07	15.68	0.00
Full	3.83	0.31	4.14	11.53
Partial	2.94	0.31	3.26	12.42
Fillet	0.00	0.00	0.00	15.68

6.4 Through thickness properties:

Calculation according to Ec3, table shown in Appendix C.

Assuming Z_{Rd} is equal for all plates.

The original design was preheated, and this was used in the calculations.

Formula used (14):

$$Z_{Ed} = Z_a + Z_b + Z_c + Z_d + Z_e$$

Original design:

$$Z_{Ed} = 9+8+8+0-8 = \underline{17}$$

Full and partial penetration designs:

$$Z_{Ed} = 9+5+8+3-8 = \underline{17}$$

Fillet design:

$$Z_{Ed} = 9+0+8+3-8 = \underline{12}$$

7.0 Comments to Results

The stresses from the hot-spot method showed very little variation, it can be assumed that the structural stress concentration is the main effect for the stress concentration in the hot-spot method when the structure is of high stiffness. Therefore, for stiff structures, the modeling of the weld can be neglected for hot-spot method. Although DNV recommends modeling with a weld because of the extra stiffness and it doesn't require much effort.

In the notch-stress method the effect of weld design is clearly shown as the stresses varies from design to design. DNV suggests notch-stress method for checking different weld geometry (8). Where there is high geometric stress because of the weld toe, the hot-spot method gives a lower stress than the notch-stress method. To get the most conservative result, notch stress is recommended.

Because of the high risk environment the weld should be available to for inspection according to standards. But, because of the high stress concentration at the left toe, for most weld designs, the crack will most likely initiate at here, shown in figure 43. Could use other design based on this.

However, the potential for root cracking has to be checked, and the only method for this in this case is the use of the notch-stress method. Since this requires some extra time modeling, approximately 40 minutes, which is higher than the time saved on manufacturing, 16 minutes for fillet weld, 12 minutes for partial-penetrating weld (estimate), it is not recommended to do so.

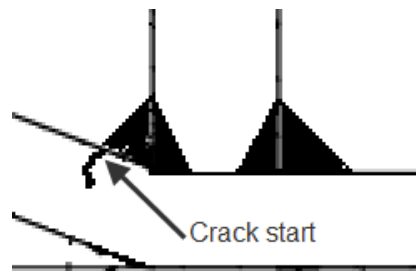


Figure 42: Most likely place of crack start because of the highest stress concentrations

For fillet welds the stress at the root is too high to neglect the chance of crack start at the root. Since this area is unavailable, it will be hard to detect under later inspections.

Partial penetration welds should be sufficient to use, the magnitude of the stresses at the root is quite low. The probability of failure based on fatigue damage accumulated, according to DNV, is 0.000001 which is quite low. And for $DFF = 10$, $D = 0.5$ shows that the risk is low.

There are few advantages choosing a different design. The effect of misalignment is neglectable for the alternative designs, for the original design it is recommended to use k_m of 1.1 as default in the stress calculation (9). The total strength in an accident limit state would not be decreased in the original design, since the weld is "as strong as the parent material" (1). Only the fillet design show better trough thickness properties ($Z_{Ed}=12$)

Because the stiffener is a part of the load bracket distributing the load to the beams, a few problems regarding welding in the transition between the plates might occur. These are not discussed in this thesis.

8.0 Conclusion

For the mentioned reasons in “comments on results” the original weld design seems to be the best choice.

For offshore structures fatigue and risk managements seems to be the most important factor regarding weld design. In high risk environment load carrying welds should always be full penetrating (8). Non-load carrying welds needs to be checked for probability of root failure. Especially important if the weld is a part of the structure redundancy. Inspections reduces the probability of unexpected failure, therefore welds made unavailable should be designed for lower chance of fatigue failure.

If in doubt, the notch stress method should be used. For most accurate results the weld should be modeled in the most realistic manner as possible, since the notch effect is dependent on weld geometry. 11% difference in stress results and 40% difference in accumulated fatigue damage results were shown in the example in this thesis.

With increasing computer power and easy modeling programs with FEA subprograms, it is quite easy and fast to check the notch stress. Of course this is dependent on the size of the model. Local checks are recommended if in doubt.

If better fatigue properties are needed, weld preparation could be made, and modeled into the analysis (8). Studies show that a FAT300 curve could be used for high quality welds with weld preparations and modeled notch (11)

However, with engineering cost in mind, if it is not critical for a specific weld, a standard weld should be used. If it is a series produced component or many components the extra cost of engineering is likely be justified.

Other than this, it is unlikely that there is much time and money to save by doing a notch stress analysis.

8.1 Flow chart for choosing weld type

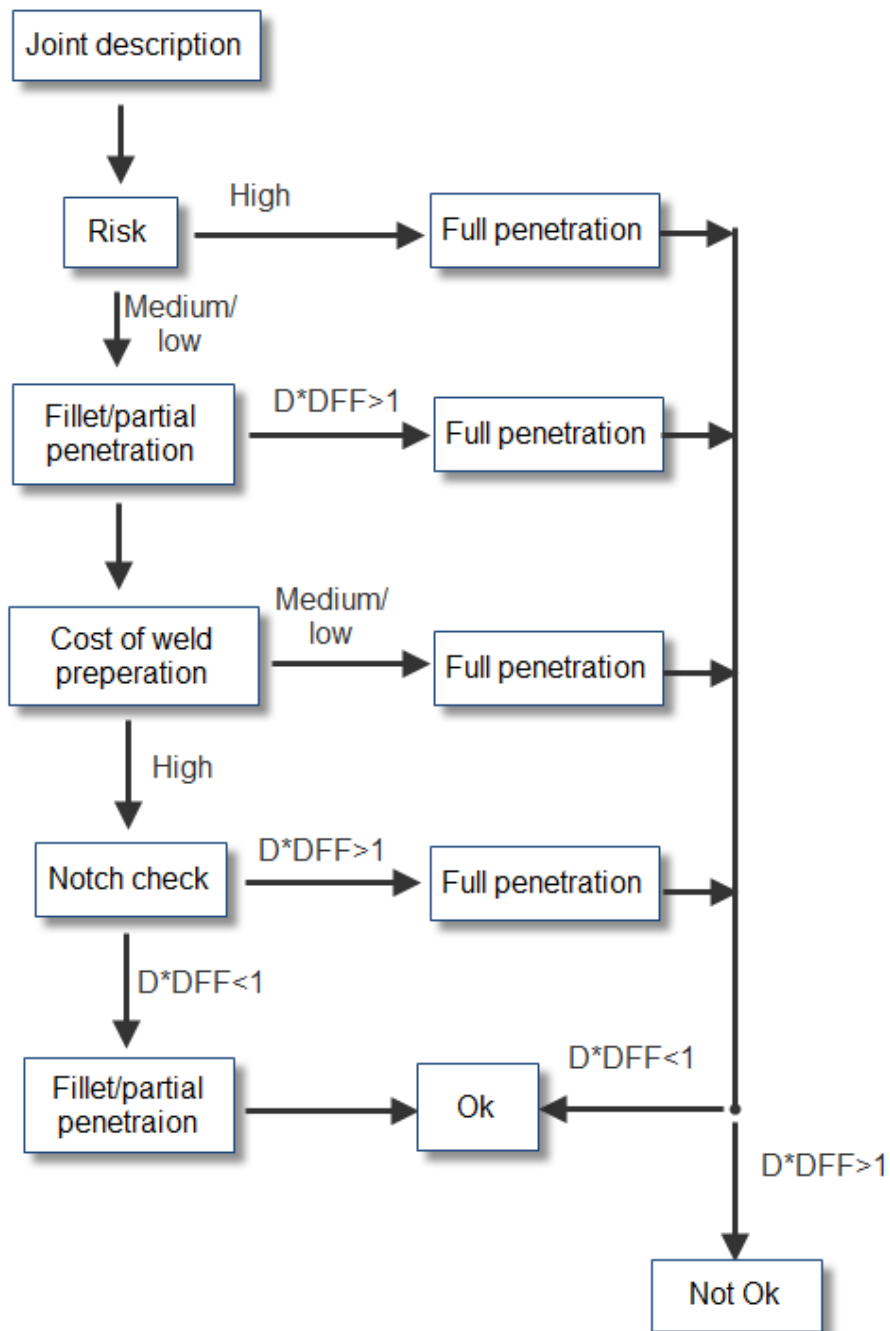


Figure 43: Suggested flowchart for choosing weld type

Commentary for flowchart:

The flowchart is based on a weld geometry which is not represented by a nominal reference curve. If the weld can be identified in a standard by the detail classification, and $D \cdot DFF < 1$ for the nominal approach, this is sufficient. Further analysis can then be neglected, stop at cost of weld preparation.

Risk is based on probability*consequence, and probability is reduced when welds can be inspected in-service, better weld quality and more detailed analysis.

If ending up at "Not Ok", alternating design should be considered.

8.2 Further work

Better cost estimation with design in mind, how much weld preparation need to be done before the extra check of notch stress on fillets weld can be justified. A quick estimate after the models used here, 40 min modeling time divided by 6.32 min/m preparation time for reference thickness of 30 mm, would give approximately 6.33m of plates before preparation time equals modeling time. The cost of preparation is most likely cheaper than the cost of engineering which also needs to be considered.

To decrease engineering time, better mesh control tools could be developed. For example enforce 3 layers of unaltered mesh from a notch surface, and control the ratio of the mesh size growth after.

Should be noted that the current automated mesh control tool for Solidworks was tested, it often created large models and errors. It was also not possible to control the mesh to match the mesh according to standards.

Automated mesh function for hot-spot and notch stress could be made, with automated fatigue testing in programs, and testing these in relation to existing models and test data.

Alternatively a proper procedure for design of notch-stress or hot-spot analysis could be made.

Check if flow chart is usable and develop it further.

Consider allowing design for controlled crack start in standards.

9.0 References

1. **Maddox, S.J.** *Fatigue Strength of Welded Structures 2nd edition*. Cambridge : Abington Publishing, 1991.
2. **Jármai, K. and Farkas, J.** Cost calculation and optimisation of welded steel structures. [book auth.] Elsevier. *Journal of Constructional Steel Research* 50 (115–135). Miskolc, Hungary : Elsevier, 1999.
3. **Rangachari Narayanan, V. Kalyanaraman, A.R. Santhakumar, S.Seetharaman, S.R. Satish Kumar, S. Arul Jayachandran, R. Senthil.** Teaching Materials - Contents. *INSDAG*. [Online] INSTITUTE FOR STEEL DEVELOPMENT & GROWTH, 2011. [Cited: April 18, 2013.] http://www.steel-insdag.org/TM_Contents.asp.
4. **Anderson, T.L.** *Fracture Mechanics Fundamental and Applications*. s.l. : Taylor and Francis Group, 2005.
5. **Fricke, W.** Fatigue strength assessment of local stresses in welded joints. [book auth.] Kenneth A. Macdonald. *Fracture and fatigue of welded joints and structures*. Cambridge : Woodhead Publishing Limited, 2011.
6. **Luo, Yu, Ishiyama, Morinobu and Murakawa, Hidekazu.** *Welding Deformation Of Plates with Longitudinal Curvature*. Osaka : Joining and Welding Research Institute of Osaka University, 1999.
7. **Maddox, S.J.** Fatigue design rules for welded structures. [book auth.] Kenneth A. Macdonald. *Fracture and fatigue of welded joints and structures*. Cambridge : Woodhead Publishing Limited, 2011.
8. **DNV.** DNV Service Specifications, Standards and Recommended Practices. *DNV*. [Online] February 1, 2012. [Cited: April 5, 2013.] http://exchange.dnv.com/publishing/Codes/ToC_edition.asp#Recommended_Practices. DNV-RP-C203.
9. **Hobbacher, A.** *Recommendations for Fatigue Design of Welded Joints and Component*. [Best Practice Documents] Paris : International Institute of Welding, 2008. IIW document IIW-1823-07 ;XIII-2151r4-07;XV-1254r4-07.
10. *Eurocode 3: Design of steel structures, Part 1-9: Fatigue*. **NS-EN. 9**, s.l. : Standard Norge, 2005: +NA2010, Vol. 1. NS-EN 1993-1-9:2005+NA:2010.
11. **Pedersen, M.M., et al.** Experience with the Notch Stress Approach for Fatigue Assessment of Welded Joints. Borlänge, Sweden : Proceedings of the Swedish Conference on Light Weight Optimized Welded Structures, 2010.
12. **Aygül, Mustafa.** *Fatigue Analysis of Welded Structures Using the Finite Element Method* . Gothenburg : Chalmers University of Technology , 2012.
13. **Fricke, Wolfgang.** *IIW Recommendations for the Fatigue Assessment by Notch Stress Analysis for Welded Structures*. Hamburg : International Institute of Welding, 2010. IIW-Doc. XIII-2240r2-08/XV-1289r2-08.
14. *Eurocode 3: Design of steel structures, Part 1-10 Material toughness and through-thickness properties*. **NS-EN. 10**, s.l. : Standard Norge, 2009, Vol. 1. NS-EN 1993-1-10:2005/AC:2009.
15. **ABS.** Guide for The Fatigue Assessment of Offshore Structures. *American Bureau of Shipping*. [Online] November 2010. [Cited: June 10, 2013.] http://www.eagle.org/eagleExternalPortalWEB/?_nfpb=true&_pageLabel=abs_eagle_portal_marine_rules_guides_book. 115.
16. **DNV.** DNV Service Specifications, Standards and Recommended Practices. *DNV*. [Online] Det Norske Veritas, April 1, 2011. [Cited: April 5, 2013.] http://exchange.dnv.com/publishing/Codes/ToC_edition.asp. DNV-OS-C101.
17. **ndt-ed.org.** About NDT. *NDT Resource Center*. [Online] 1 1, 2013. [Cited: 6 14, 2013.] <http://www.ndt-ed.org/AboutNDT/aboutndt.htm>.
18. **Miller, K. Duane.** Consider the cost of joint preparation when specifying weld type. *Practical Cost-Saving Ideas for the Design Professionals: Welding*. [Online] 1997. [Cited: June 10, 2013.] <http://www.aisc.org/bookstore/itemRedirector.aspx?id=14972>.
19. **Chayoukhi, Slah.** Cost estimation of joints preparation for GMAW welding process using feature model. [book auth.] Elsevier. *Journal of materials processing technology* 199 402-411. Tunis, Tunisia : Elsevier, 2007.
20. **Solidworks.** Solidworks Help. [Online] Dassault Systèmes, 2013. <http://help.solidworks.com/>.

10.0 Appendices

Note:

- Because of the high amount of data, instead of listing results, stress is shown in screenshot with maximum stress extrapolated.

10.1 Appendix A: Stress extrapolation and fatigue damage calculations for Hot-Spot method

The calculations are done as mentioned in chapter 5.6, and calculated as follow:

Detail category for S-N curve:

$$\Delta\sigma_c := 90\text{MPa}$$

Load function:

$$F_u(i) := \left[\begin{aligned} & \left[\left(\frac{i-1}{2} \right) \cdot W_p \cdot \sigma_n(i) + (W_{\text{topdrive}} + W_{\text{traverse}} + W_p) \right] x(i) \dots \\ & + \left[\left(\frac{2 \cdot n_{p.\text{max}} - i}{2} \right) \cdot W_p \cdot \sigma_n(i+1) + (W_{\text{topdrive}} + W_{\text{traverse}} + W_p) \right] y(i) \dots \\ & + (W_{\text{topdrive}} + W_{\text{traverse}} + W_p) \cdot z(i) \end{aligned} \right]$$

Function for N(i)

$$N(i) := \text{round} \left[N \left[\frac{F_u(i)}{F_u(n_{p.\text{max}})} \cdot (\gamma_{\text{Ff}} \cdot \Delta\sigma_{\text{max}}) \right] \right]$$

Partial load factor for Fatigue limit state:

$$\gamma_{\text{Ff}} := 1.0$$

Number of times direct stress load (i) is experienced for trough life (reference internal load history):

$$n_i := 300$$

Accumulated fatigue damage D:

$$D := \sum_{i=1}^{2n_{p.\text{max}}+1} \frac{n_i}{N(i)}$$

10.1.2 Weld design 1

Figure A.1 showing extrapolation of maximum 1st principle stress at the intersection lines 1.5t: 119.4MPa and 0.5t: 136.6MPa.

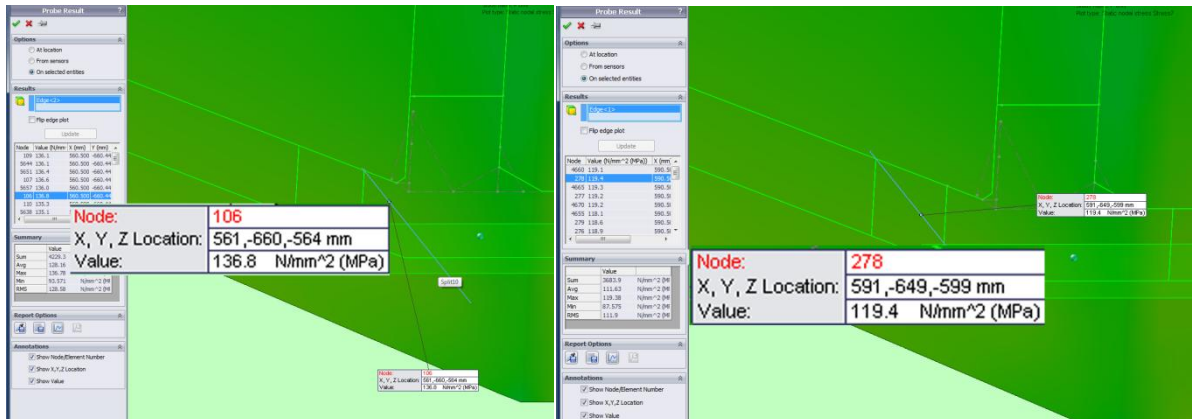


Figure A. 1: Maximum 1st principle stress at distances 0.5t (left) and 1.5t (right) from the weld toe

Calculated damage for the interpolation method (a):

Extrapolated stress σ_1 , at 0.5t and 1.5t:

$$\sigma_{0.5t} := 136.8 \cdot \text{MPa}$$

$$\sigma_{1.5t} := 119.4 \cdot \text{MPa}$$

Maximum effective stress

$$\sigma_{\text{eff}} := \sigma_{1.5t} + (\sigma_{0.5t} - \sigma_{1.5t}) \cdot \frac{-1.5}{0.5 - 1.5}$$

$$\sigma_{\text{eff}} = 145.5 \cdot \text{MPa}$$

Maximum stress amplitude

$$\Delta\sigma_{\text{max}} := \sigma_{\text{eff}} \cdot \frac{F_u(n_{p,\text{max}}) - F_u(1)}{F_u(n_{p,\text{max}})} = 139.229 \cdot \text{MPa}$$

$$D := \sum_{i=1}^{2n_{p,\text{max}}+1} \frac{n_i}{N(i)}$$

$$D = 0.10$$

Calculated damage for factor method (b):

Extrapolated stress σ_1 , at 0.5t:

$$\sigma_{0.5t} := 136.6 \text{ MPa}$$

Calculated maximum effective stress

$$\sigma_{\text{eff}} := 1.12 \cdot \sigma_{0.5t}$$

$$\sigma_{\text{eff}} = 152.992 \text{ MPa}$$

Maximum stress amplitude

$$\Delta\sigma_{\text{max}} := \sigma_{\text{eff}} \cdot \frac{F_u(n_{p,\text{max}}) - F_u(1)}{F_u(n_{p,\text{max}})} = 144.609 \text{ MPa}$$

$$D := \sum_{i=1}^{2n_{p,\text{max}}+1} \frac{n_i}{N(i)}$$

$$D = 0.12$$

10.1.2 Weld design 2

Figure A.2 showing extrapolation of maximum 1st principle stress at the intersection lines 1.5t: 118.6MPa and 0.5t: 138.5MPa.

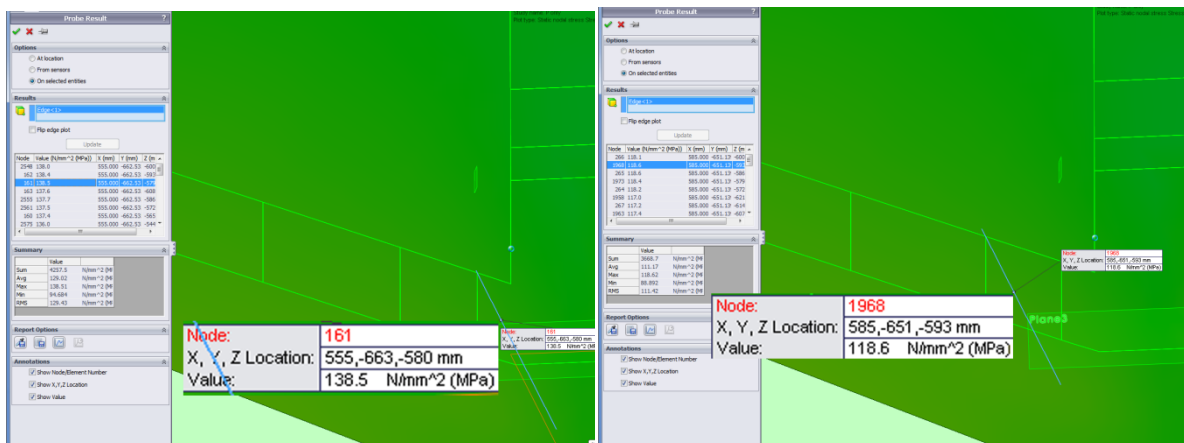


Figure A. 2: Maximum 1st principle stress at distances 0.5t (left) and 1.5t (right) from the weld toe

Calculated damage for the interpolation method (a):

Extrapolated stress σ_1 , at 0.5t and 1.5t:

$$\sigma_{0.5t} := 138.5 \cdot \text{MPa}$$

$$\sigma_{1.5t} := 118.6 \cdot \text{MPa}$$

Maximum effective stress

$$\sigma_{\text{eff}} := \sigma_{1.5t} + (\sigma_{0.5t} - \sigma_{1.5t}) \cdot \frac{-1.5}{0.5 - 1.5}$$

$$\sigma_{\text{eff}} = 148.45 \cdot \text{MPa}$$

Maximum stress amplitude

$$\Delta\sigma_{\text{max}} := \sigma_{\text{eff}} \cdot \frac{F_u(n_{p.\text{max}}) - F_u(1)}{F_u(n_{p.\text{max}})} = 140.316 \cdot \text{MPa}$$

$$D := \sum_{i=1}^{2n_{p.\text{max}}+1} \frac{n_i}{N(i)}$$

$$D = 0.10$$

Calculated damage for factor method(b):

Extrapolated stress σ_1 , at 0.5t:

$$\sigma_{0.5t} := 138.5 \cdot \text{MPa}$$

Calculated maximum effective stress

$$\sigma_{\text{eff}} := 1.12 \cdot \sigma_{0.5t}$$

$$\sigma_{\text{eff}} = 155.12 \cdot \text{MPa}$$

Maximum stress amplitude

$$\Delta\sigma_{\text{max}} := \sigma_{\text{eff}} \cdot \frac{F_u(n_{p.\text{max}}) - F_u(1)}{F_u(n_{p.\text{max}})} = 146.62 \cdot \text{MPa}$$

$$D := \sum_{i=1}^{2n_{p.\max}+1} \frac{n_i}{N(i)}$$

$$D = 0.12$$

10.1.2 Weld design 2

Figure A.3 showing extrapolation of maximum 1st principle stress at the intersection lines 1.5t: 120.3MPa and 0.5t: 136.8MPa.

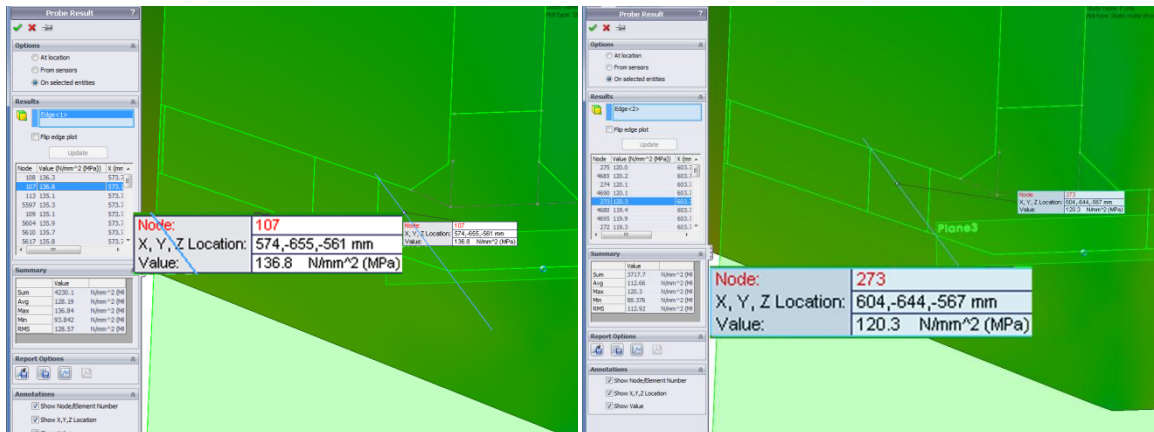


Figure A. 3: Maximum 1st principle stress at distances 0.5t (left) and 1.5t (right) from the weld toe

Calculated damage for the interpolation method (a):

Extrapolated stress σ_1 , at 0.5t and 1.5t:

$$\sigma_{0.5t} := 136.8 \cdot \text{MPa}$$

$$\sigma_{1.5t} := 120.3 \cdot \text{MPa}$$

Maximum effective stress

$$\sigma_{\text{eff}} := \sigma_{1.5t} + (\sigma_{0.5t} - \sigma_{1.5t}) \cdot \frac{-1.5}{0.5 - 1.5}$$

$$\sigma_{\text{eff}} = 145.05 \cdot \text{MPa}$$

Maximum stress amplitude

$$\Delta\sigma_{\max} := \sigma_{\text{eff}} \cdot \frac{F_u(n_{p.\max}) - F_u(1)}{F_u(n_{p.\max})} = 137.102 \cdot \text{MPa}$$

$$D := \sum_{i=1}^{2n_{p,max}+1} \frac{n_i}{N(i)}$$

$$D = 0.10$$

Calculated damage for factor method (b):

Extrapolated stress σ_1 , at 0.5t:

$$\sigma_{0.5t} := 136.8 \cdot \text{MPa}$$

Calculated maximum effective stress

$$\sigma_{\text{eff}} := 1.12 \cdot \sigma_{0.5t}$$

$$\sigma_{\text{eff}} = 153.216 \cdot \text{MPa}$$

Maximum stress amplitude

$$\Delta\sigma_{\text{max}} := \sigma_{\text{eff}} \cdot \frac{F_u(n_{p,max}) - F_u(1)}{F_u(n_{p,max})} = 144.821 \cdot \text{MPa}$$

$$D := \sum_{i=1}^{2n_{p,max}+1} \frac{n_i}{N(i)}$$

$$D = 0.12$$

10.1.4 Weld design 4

Figure A.4 showing extrapolation of maximum 1st principle stress at the intersection lines 1.5t: 118.9MPa and 0.5t: 136.6MPa.

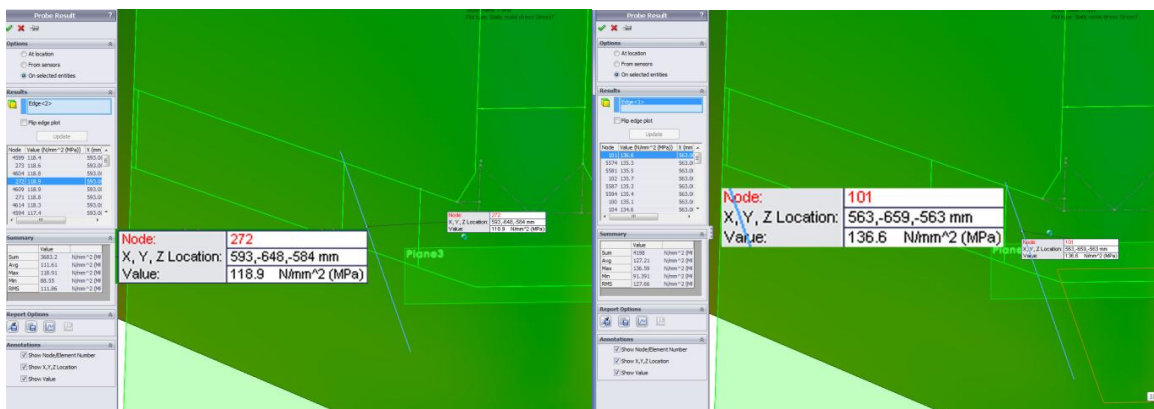


Figure A. 4: Maximum 1st principle stress at distances 0.5t (left) and 1.5t (right) from the weld toe

Calculated damage for the interpolation method (a):

Extrapolated stress σ_1 , at 0.5t and 1.5t:

$$\sigma_{0.5t} := 136.6 \cdot \text{MPa}$$

$$\sigma_{1.5t} := 118.9 \cdot \text{MPa}$$

Maximum effective stress

$$\sigma_{\text{eff}} := \sigma_{1.5t} + (\sigma_{0.5t} - \sigma_{1.5t}) \cdot \frac{-1.5}{0.5 - 1.5}$$

$$\sigma_{\text{eff}} = 145.45 \cdot \text{MPa}$$

Maximum stress amplitude

$$\Delta\sigma_{\text{max}} := \sigma_{\text{eff}} \cdot \frac{F_u(n_{p.\text{max}}) - F_u(1)}{F_u(n_{p.\text{max}})} = 137.48 \cdot \text{MPa}$$

$$D := \sum_{i=1}^{2n_{p.\text{max}}+1} \frac{n_i}{N(i)}$$

$$D = 0.10$$

Calculated damage for factor method (b):

Extrapolated stress σ_1 , at 0.5t:

$$\sigma_{0.5t} := 136.6 \cdot \text{MPa}$$

Calculated maximum effective stress

$$\sigma_{\text{eff}} := 1.12 \cdot \sigma_{0.5t}$$

$$\sigma_{\text{eff}} = 152.992 \cdot \text{MPa}$$

Maximum stress amplitude

$$\Delta\sigma_{\text{max}} := \sigma_{\text{eff}} \cdot \frac{F_u(n_{p.\text{max}}) - F_u(1)}{F_u(n_{p.\text{max}})} = 144.609 \cdot \text{MPa}$$

$$D := \sum_{i=1}^{2n_{p.\text{max}}+1} \frac{n_i}{N(i)}$$

$$D = 0.12$$

10.2 Appendix B: Stress extrapolation and fatigue damage calculations for Notch-stress method

The calculations are done as mentioned in 5.6

Detail category for S-N curve:

$$\Delta\sigma_c := 225\text{MPa}$$

Load function:

$$F_u(i) := \left[\left[\left(\frac{i-1}{2} \right) \cdot W_p \cdot \text{on}(i) + (W_{\text{topdrive}} + W_{\text{traverse}} + W_p) \right] x(i) \dots \right. \\ \left. + \left[\left(\frac{2 \cdot n_{p.\text{max}} - i}{2} \right) \cdot W_p \cdot \text{on}(i+1) + (W_{\text{topdrive}} + W_{\text{traverse}} + W_p) \right] y(i) \dots \right. \\ \left. + (W_{\text{topdrive}} + W_{\text{traverse}} + W_p) \cdot z(i) \right]$$

Function for N(i)

$$N(i) := \text{round} \left[N \left[\frac{F_u(i)}{F_u(n_{p.\text{max}})} \cdot (\gamma_{\text{Ff}} \cdot \Delta\sigma_{\text{max}}) \right] \right]$$

Partial load factor for Fatigue limit state:

$$\gamma_{\text{Ff}} := 1.0$$

Number of times direct stress load (i) is experienced for trough life (reference internal load history):

$$n_i := 300$$

Accumulated fatigue damage D:

$$D := \sum_{i=1}^{2n_{p.\text{max}}+1} \frac{n_i}{N(i)}$$

10.2.1 Weld design 1

Figure B.1 showing extrapolation of maximum 1st principle stress at the notch surface of the most critical weld toe, 435.8MPa



Figure B. 1: Maximum 1st principle stress

Maximum effective stress

$$\sigma_{\text{eff}} := 435.8 \cdot \text{MPa}$$

Maximum stress amplitude

$$\Delta\sigma_{\text{max}} := \sigma_{\text{eff}} \cdot \frac{F_u(n_{p.\text{max}}) - F_u(1)}{F_u(n_{p.\text{max}})} = 411.92 \cdot \text{MPa}$$

$$D := \sum_{i=1}^{2n_{p.\text{max}}+1} \frac{n_i}{N(i)}$$

$$D = 0.18$$

10.2.2 Weld design 2

Figures B.2 showing extrapolation of maximum 1st principle stress at the notch surface of the most critical weld toe, 415.7MPa



Figure B. 2: Maximum 1st principle stress

Maximum effective stress

$$\sigma_{\text{eff}} := 415.7 \cdot \text{MPa}$$

Maximum stress amplitude

$$\Delta\sigma_{\text{max}} := \sigma_{\text{eff}} \cdot \frac{F_u(n_{p.\text{max}}) - F_u(1)}{F_u(n_{p.\text{max}})} = 392.922 \cdot \text{MPa}$$

$$D := \sum_{i=1}^{2n_{p.\text{max}}+1} \frac{n_i}{N(i)}$$

$$D = 0.15$$

10.2.3 Weld design 3

Figures B.3 showing extrapolation of maximum 1st principle stress at the notch surface of the most critical weld toe, 462.9MPa

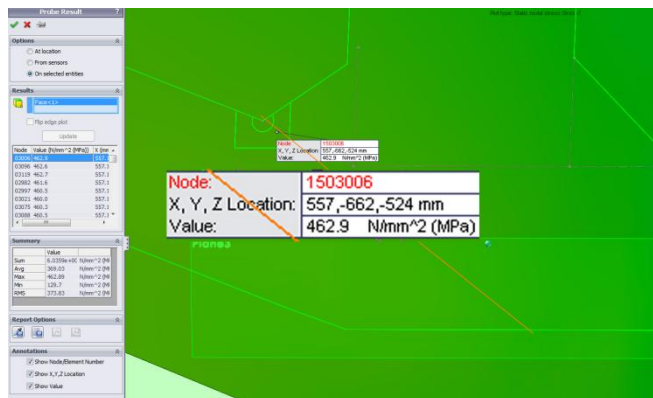


Figure B. 3: Maximum 1st principle stress

Maximum effective stress

$$\sigma_{\text{eff}} := 462.9 \cdot \text{MPa}$$

Maximum stress amplitude

$$\Delta\sigma_{\text{max}} := \sigma_{\text{eff}} \cdot \frac{F_u(n_{p.\text{max}}) - F_u(1)}{F_u(n_{p.\text{max}})} = 437.535 \cdot \text{MPa}$$

$$D := \sum_{i=1}^{2n_{p,max}+1} \frac{n_i}{N(i)}$$

$$D = 0.21$$

10.2.4 Weld design 4

Figures B.4 showing extrapolation of maximum 1st principle stress at the notch surface of the most critical weld toe, 426.6MPa

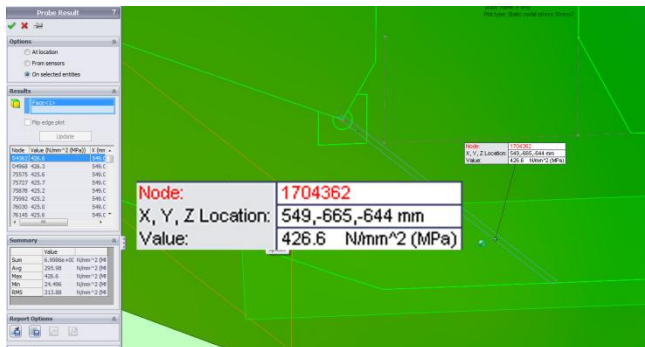


Figure B. 4: Maximum 1st principle stress

Maximum effective stress

$$\sigma_{\text{eff}} := 426.6 \text{ MPa}$$

Maximum stress amplitude

$$\Delta\sigma_{\text{max}} := \sigma_{\text{eff}} \cdot \frac{F_u(n_{p,max}) - F_u(1)}{F_u(n_{p,max})} = 403.224 \text{ MPa}$$

$$D := \sum_{i=1}^{2n_{p,max}+1} \frac{n_i}{N(i)}$$

$$D = 0.16$$

10.2.5 Weld design 5

Figures B.5 showing extrapolation of maximum 1st principle stress at the notch surface of the most critical weld root, 380.4MPa

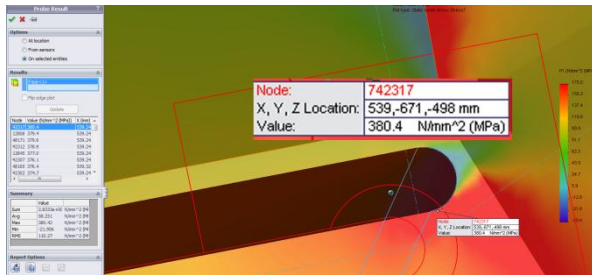


Figure B. 5: Maximum 1st principle stress

Maximum effective stress

$$\sigma_{\text{eff}} := 380.4 \text{ MPa}$$

Maximum stress amplitude

$$\Delta\sigma_{\text{max}} := \sigma_{\text{eff}} \cdot \frac{F_u(n_{p,\text{max}}) - F_u(1)}{F_u(n_{p,\text{max}})} = 359.556 \text{ MPa}$$

$$D := \sum_{i=1}^{2n_{p,\text{max}}+1} \frac{n_i}{N(i)}$$

$$D = 0.12$$

10.2.6 Weld design 6

Figures B.1 showing extrapolation of maximum 1st principle stress at the notch surface of the most critical weld toe, 285.0MPa

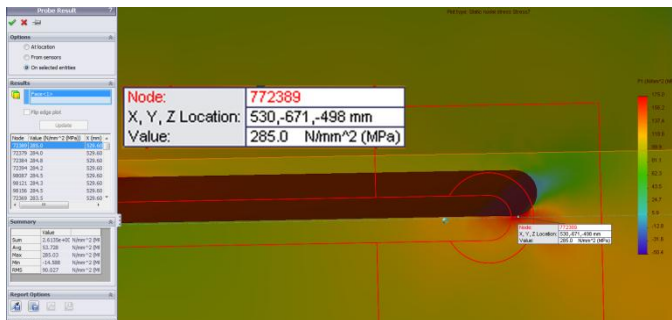


Figure B. 6: Maximum 1st principle stress

Maximum effective stress

$$\sigma_{\text{eff}} := 285 \cdot \text{MPa}$$

Maximum stress amplitude

$$\Delta\sigma_{\text{max}} := \sigma_{\text{eff}} \cdot \frac{F_{\text{u}}(n_{\text{p.max}}) - F_{\text{u}}(1)}{F_{\text{u}}(n_{\text{p.max}})} = 269.383 \cdot \text{MPa}$$

$$D := \sum_{i=1}^{2n_{\text{p.max}}+1} \frac{n_i}{N(i)}$$

$$D = 0.05$$

10.3 Appendix C: Through thickness reference table

EN 1993-1-10 : 2005 (E)

Table 3.2: Criteria affecting the target value of Z_{Ed}



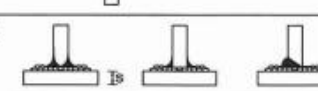

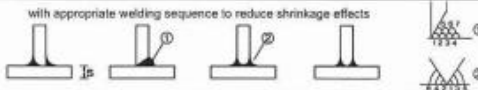
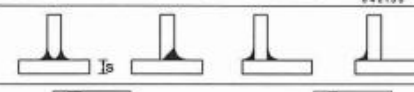

a)	Weld depth relevant for straining from metal shrinkage	Effective weld depth a_{eff} (see Figure 3.2) = throat thicken. a of fillet welds		Z_{t1}
		$a_{eff} \leq 7\text{mm}$	$a = 5\text{ mm}$	$Z_{t2} = 0$
$7 < a_{eff} \leq 10\text{mm}$	$a = 7\text{ mm}$	$Z_{t2} = 3$		
$10 < a_{eff} \leq 20\text{mm}$	$a = 14\text{ mm}$	$Z_{t2} = 6$		
$20 < a_{eff} \leq 30\text{mm}$	$a = 21\text{ mm}$	$Z_{t2} = 9$		
$30 < a_{eff} \leq 40\text{mm}$	$a = 28\text{ mm}$	$Z_{t2} = 12$		
$40 < a_{eff} \leq 50\text{mm}$	$a = 35\text{ mm}$	$Z_{t2} = 15$		
$50 < a_{eff}$	$a > 35\text{ mm}$	$Z_{t2} = 15$		
b)	Shape and position of welds in T- and cruciform- and corner-connections		$Z_b = -25$	
		corner joints 	$Z_b = -10$	
		single run fillet welds $Z_a = 0$ or fillet welds with $Z_a > 1$ with buttering with low strength weld material 	$Z_b = -5$	
		multi run fillet welds 	$Z_b = 0$	
		partial and full penetration welds with appropriate welding sequence to reduce shrinkage effects 	$Z_b = 3$	
		partial and full penetration welds 	$Z_b = 5$	
		corner joints 	$Z_b = 8$	
c)	Effect of material thickness s on restraint to shrinkage	$s \leq 10\text{mm}$	$Z_c = 2^*$	
		$10 < s \leq 20\text{mm}$	$Z_c = 4^*$	
		$20 < s \leq 30\text{mm}$	$Z_c = 6^*$	
		$30 < s \leq 40\text{mm}$	$Z_c = 8^*$	
		$40 < s \leq 50\text{mm}$	$Z_c = 10^*$	
		$50 < s \leq 60\text{mm}$	$Z_c = 12^*$	
		$60 < s \leq 70\text{mm}$	$Z_c = 15^*$	
$70 < s$	$Z_c = 15^*$			
d)	Remote restraint of shrinkage after welding by other portions of the structure	Low restraint: Free shrinkage possible (e.g. T-joints)	$Z_d = 0$	
		Medium restraint: Free shrinkage restricted (e.g. diaphragms in box girders)	$Z_d = 3$	
		High restraint: Free shrinkage not possible (e.g. stringers in orthotropic deck plates)	$Z_d = 5$	
e)	Influence of preheating	Without preheating	$Z_e = 0$	
		Preheating $\geq 100^\circ\text{C}$	$Z_e = -8$	
* May be reduced by 50% for material stressed, in the through-thickness direction, by compression due to predominantly static loads.				



Figure C. 3: Table 3.2 showing trough thickness criteria and definition of a_{eff} (14)

10.4 Appendix D: Modeling of root for Fillet weld and Partial penetrating weld

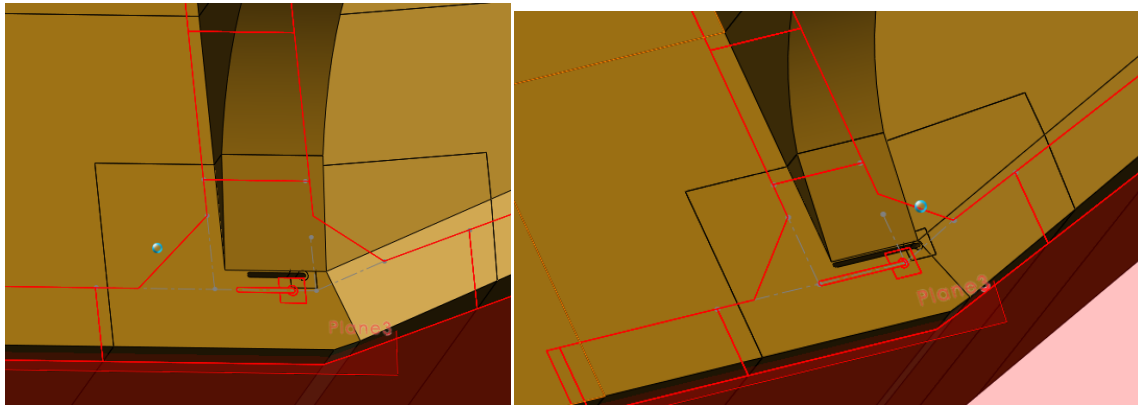


Figure D. 1: Modeling of root for fillet and partial penetrating weld in Solidworks

10.5 Appendix E: Validation of notch-stress

Comments:

- Model after DNV (8).
- Validation results show that meshing was ok.

10.5.1 Full-penetration cruciform joint

t=16 mm and "a" = 8 mm

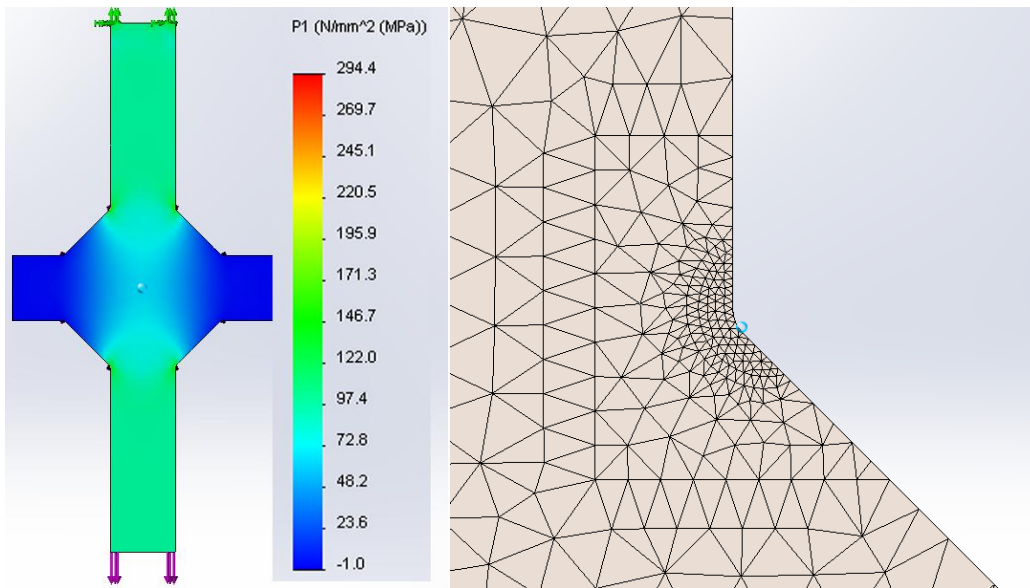


Figure E. 2: Maximum 1st principle stress and mesh geometry

Maximum effective stress

$$\sigma_{\text{eff}} := 294.4 \cdot \text{MPa}$$

Maximum stress amplitude

$$\Delta\sigma_{\text{max}} := \sigma_{\text{eff}} \cdot \frac{F_u(n_{p.\text{max}}) - F_u(1)}{F_u(n_{p.\text{max}})} = 278.268 \cdot \text{MPa}$$

$$D := \sum_{i=1}^{2n_{p,max}+1} \frac{n_i}{N(i)}$$

$$D = 0.05$$

Maximum effective stress

$$\sigma_{eff} := 100 \cdot \text{MPa}$$

Detail category is used after IIW without the misalignment factor:

$$\Delta\sigma_c := 80 \text{MPa}$$

$$\Delta\sigma_{max} := \sigma_{eff} \cdot \frac{F_u(n_{p,max}) - F_u(1)}{F_u(n_{p,max})} = 94.52 \cdot \text{MPa}$$

$$D := \sum_{i=1}^{2n_{p,max}+1} \frac{n_i}{N(i)}$$

$$D = 0.05$$

10.5.1 Fillet welded cruciform joint

t=16 mm and a = 8 mm

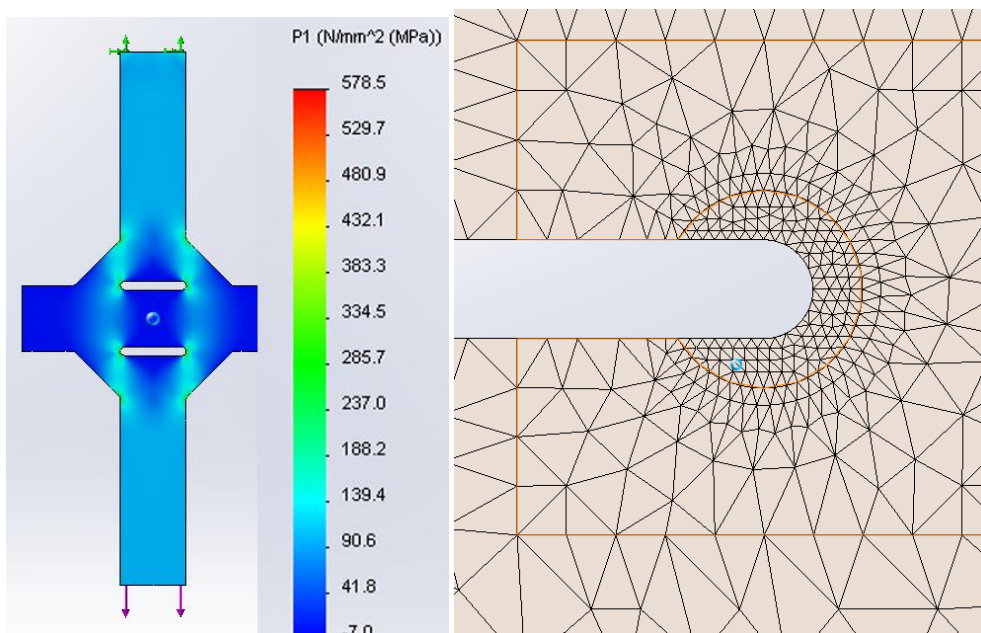


Figure E. 2: Maximum 1st principle stress and mesh geometry

Maximum effective stress

$$\sigma_{\text{eff}} := 578.5 \cdot \text{MPa}$$

Maximum stress amplitude

$$\Delta\sigma_{\text{max}} := \sigma_{\text{eff}} \cdot \frac{F_u(n_{p.\text{max}}) - F_u(1)}{F_u(n_{p.\text{max}})} = 546.801 \cdot \text{MPa}$$

$$D := \sum_{i=1}^{2n_{p.\text{max}}+1} \frac{n_i}{N(i)}$$

$$D = 0.41$$

Maximum effective stress

$$\sigma_{\text{eff}} := 100 \cdot \text{MPa}$$

Detail category is used after IIW without the misalignment factor:

$$\Delta\sigma_c := 40 \cdot \text{MPa}$$

$$\Delta\sigma_{\text{max}} := \sigma_{\text{eff}} \cdot \frac{F_u(n_{p.\text{max}}) - F_u(1)}{F_u(n_{p.\text{max}})} = 94.52 \cdot \text{MPa}$$

$$D := \sum_{i=1}^{2n_{p.\text{max}}+1} \frac{n_i}{N(i)}$$

$$D = 0.38$$

10.6 Appendix F: Comparing stress types

1st principle, von Mises and combination of perpendicular stress and shear stress
 Comments: Analysis show 1st principle stress as the highest.

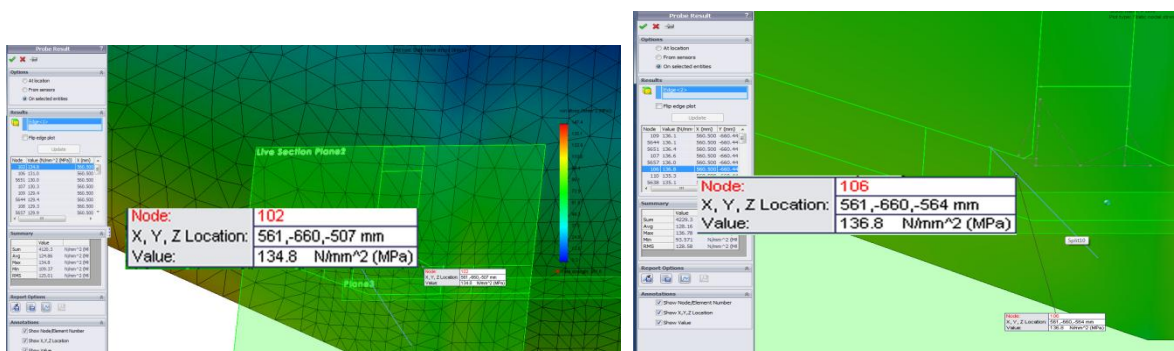


Figure F. 3: 1st principle stress (right) is slightly higher than von Mises (left) for hot-spot

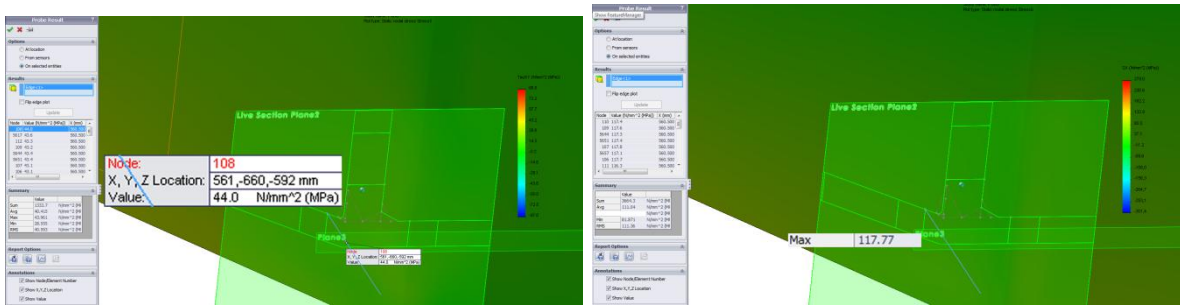


Figure F. 2: Parallel shear stress: 44MPa (left) and perpendicular stress: 117.77MPa (right)

Combination formula after DNV (8) $\sqrt{117.77^2 + 0.81 * 44^2} = 124.25MPa$
 This is lower than 1st principal stress.

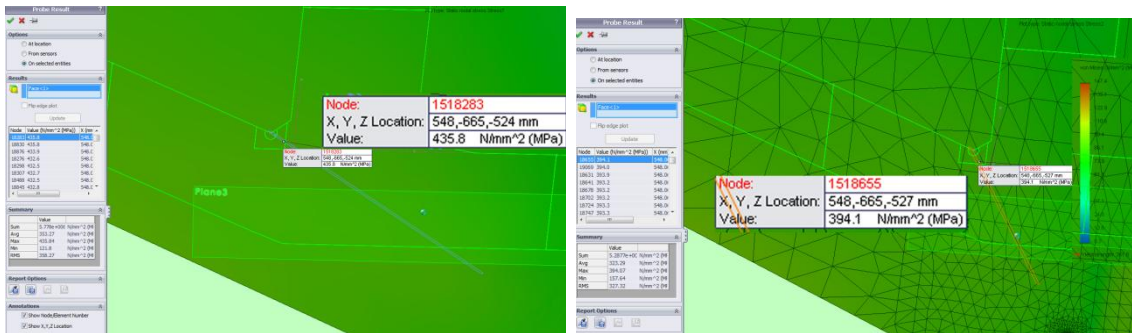


Figure F. 3: 1st principle stress (left) is slightly higher than von Mises (right) for notch-stress

10.7 Appendix G: Combination of T and P loads

P load only gives highest stresses, shown in figure G.1 to the right.

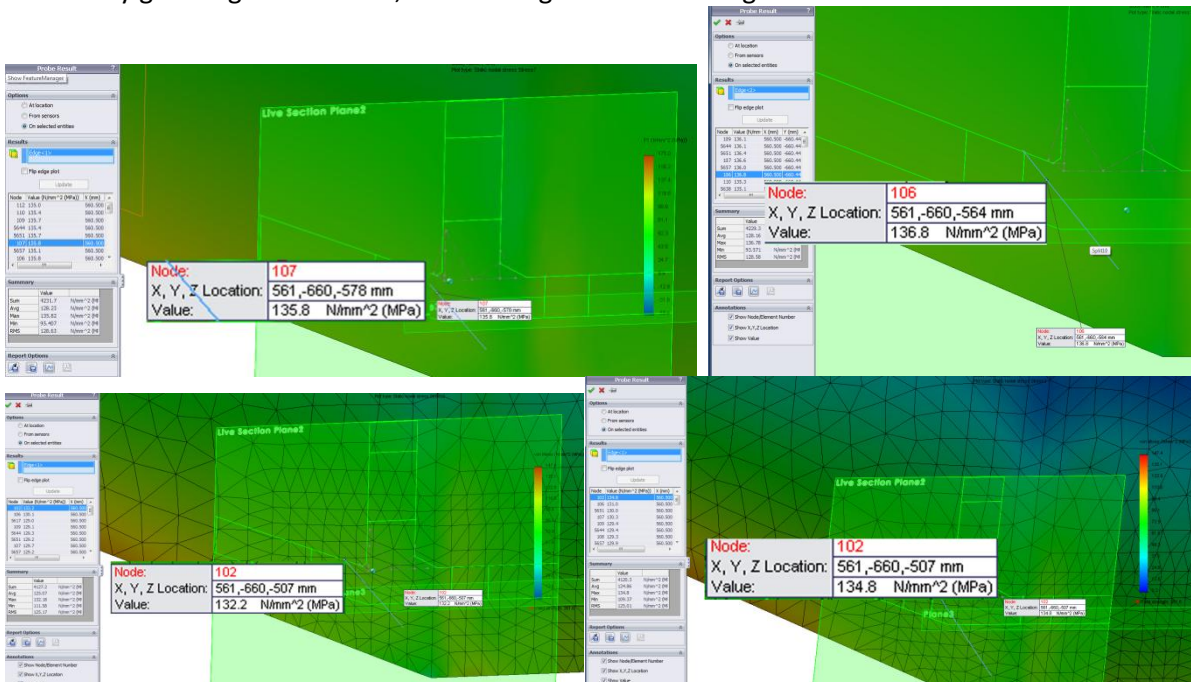


Figure G. 1: Combination of T and P loads to the left, and P load only to the right

10.8 Appendix H: Bad meshing

Volumes around the notch with radius 1.5mm and 1.75mm gave bad mesh geometry, shown in figure H.1. The effect of mesh size of 0.3mm giving lower results on maximum 1st principle stress compared to the use of mesh size of 0.25mm, shown in figure H.2.

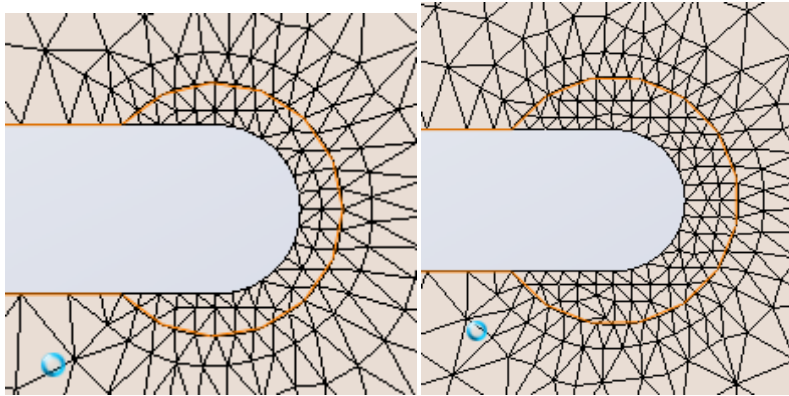


Figure H. 1: Tubular volumes around the notch with radius 1.5mm and 1.75mm showing bad mesh geometry.

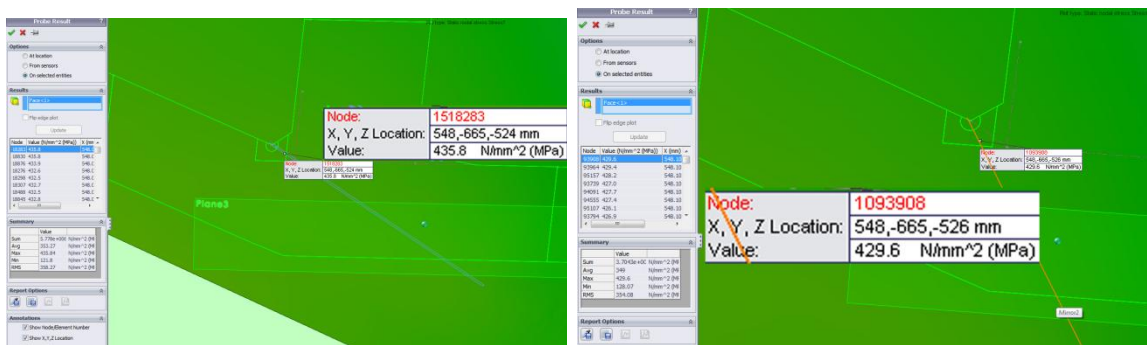


Figure H. 2: Maximum 1st principle stress for mesh size of 0.25 mm (left) and 0.3 mm (right)